

Chulalongkorn University

## Chula Digital Collections

---

Chulalongkorn University Theses and Dissertations (Chula ETD)

---

2021

### Elastic bending behaviour of sandwich composite structures with abs cores by using additive manufacturing

Dechawat Wannarong  
*Faculty of Engineering*

Follow this and additional works at: <https://digital.car.chula.ac.th/chulaetd>



Part of the [Applied Mechanics Commons](#), and the [Engineering Mechanics Commons](#)

---

#### Recommended Citation

Wannarong, Dechawat, "Elastic bending behaviour of sandwich composite structures with abs cores by using additive manufacturing" (2021). *Chulalongkorn University Theses and Dissertations (Chula ETD)*. 4778.

<https://digital.car.chula.ac.th/chulaetd/4778>

This Thesis is brought to you for free and open access by Chula Digital Collections. It has been accepted for inclusion in Chulalongkorn University Theses and Dissertations (Chula ETD) by an authorized administrator of Chula Digital Collections. For more information, please contact [ChulaDC@car.chula.ac.th](mailto:ChulaDC@car.chula.ac.th).

ELASTIC BENDING BEHAVIOUR OF SANDWICH COMPOSITE STRUCTURES WITH  
ABS CORES BY USING ADDITIVE MANUFACTURING



Mr. Dechawat Wannarong

A Thesis Submitted in Partial Fulfillment of the Requirements  
for the Degree of Master of Engineering in Mechanical Engineering

Department of Mechanical Engineering

FACULTY OF ENGINEERING

Chulalongkorn University

Academic Year 2021

Copyright of Chulalongkorn University

พฤติกรรมการณ์ดัดโค้งของโครงสร้างเชิงประกอบแบบรังผึ้ง  
ที่ขึ้นรูปด้วยกระบวนการพิมพ์ 3 มิติ



วิทยานิพนธ์นี้เป็นส่วนหนึ่งของการศึกษาตามหลักสูตรปริญญาวิศวกรรมศาสตรมหาบัณฑิต  
สาขาวิชาวิศวกรรมเครื่องกล ภาควิชาวิศวกรรมเครื่องกล  
คณะวิศวกรรมศาสตร์ จุฬาลงกรณ์มหาวิทยาลัย  
ปีการศึกษา 2564  
ลิขสิทธิ์ของจุฬาลงกรณ์มหาวิทยาลัย

Thesis Title	ELASTIC BENDING BEHAVIOUR OF SANDWICH COMPOSITE STRUCTURES WITH ABS CORES BY USING ADDITIVE MANUFACTURING
By	Mr. Dechawat Wannarong
Field of Study	Mechanical Engineering
Thesis Advisor	Associate Professor THANYARAT SINGHANART, Ph.D.

---

Accepted by the FACULTY OF ENGINEERING, Chulalongkorn University in  
Partial Fulfillment of the Requirement for the Master of Engineering

..... Dean of the FACULTY OF  
ENGINEERING  
(Professor SUPOT TEACHAVORASINSKUN, D.Eng.)

THESIS COMMITTEE

..... Chairman  
(Associate Professor Gridsada Phanomchoeng, Ph.D.)  
..... Thesis Advisor  
(Associate Professor THANYARAT SINGHANART, Ph.D.)  
..... Examiner  
(Associate Professor JIRAPONG KASIVITAMNUAY,  
D.Eng.)  
..... External Examiner  
(Sedthawatt Sucharitpwatskul, Ph.D.)

เดชาวัตร วรรณรงค์ : พฤติกรรมการดัดโค้งของโครงสร้างเชิงประกอบแบบรังผึ้งที่ขึ้นรูปด้วยกระบวนการพิมพ์ 3 มิติ. ( ELASTIC BENDING BEHAVIOUR OF SANDWICH COMPOSITE STRUCTURES WITH ABS CORES BY USING ADDITIVE MANUFACTURING) อ.ที่ปรึกษาหลัก : รศ. ดร.ธัญญารัตน์ สิงหนาท

การรักษาประสิทธิภาพของโครงสร้างแบบแซนวิชในขณะรับแรงดัดงอและความแข็งแรงของแรงดัดงอนั้นเป็นเรื่องที่ยาก ในการศึกษาครั้งนี้ได้มีการประยุกต์ใช้โครงสร้างเชิงประกอบแบบรังผึ้ง ซึ่งโครงสร้างรังผึ้งถูกขึ้นรูปด้วยกระบวนการพิมพ์ 3 มิติในหลายการออกแบบและหลายความหนาแน่นของรังผึ้ง ได้แก่โครงสร้างรังผึ้งแบบหกเหลี่ยม โครงสร้างรังผึ้งแบบรีเอ็นทรีอันท์ และโครงสร้างรังผึ้งแบบวงกลม โครงสร้างเชิงประกอบแบบรังผึ้งถูกนำไปทดสอบการดัดงอแบบ 3 จุดเพื่อศึกษาแรงดัดงอและความแข็งแรงของแรงดัดงอ พลาสติกอะครีโลไนไตรล์-บิวทาไดอีน-สไตรีนหรือเอบีเอสถูกนำมาใช้เป็นวัสดุสำหรับโครงสร้างรังผึ้ง และแผ่นคาร์บอนไฟเบอร์เส้นใยทิศทางเดียวถูกนำมาใช้เป็นแผ่นประกอบชั้นนอก จากการศึกษาค้นพบว่าโครงสร้างเชิงประกอบแบบรังผึ้งที่มีความหนาแน่นของรังผึ้งที่มาก ก็จะมีประสิทธิภาพในการรับแรงดัดงอและความแข็งแรงของแรงดัดงอได้ดีกว่าโครงสร้างเชิงประกอบแบบรังผึ้งที่มีความหนาแน่นของรังผึ้งที่น้อย นอกจากนั้นโครงสร้างรังผึ้งแบบรีเอ็นทรีอันท์สามารถรับแรงดัดงอและความแข็งแรงของแรงดัดงอได้ดีที่สุด เนื่องจากว่ามีอัตราส่วนผิวของเป็นลบ การวิเคราะห์ด้วยไฟไนต์เอลิเมนต์ถูกนำมาใช้และเปรียบเทียบกับทดสอบการดัดงอแบบ 3 จุด การศึกษานี้พบว่าการออกแบบตัวโครงสร้างรังผึ้งสามารถช่วยเพิ่มประสิทธิภาพของโครงสร้างเชิงประกอบได้ ผลลัพธ์เหล่านี้เป็นสิ่งใหม่แก่การออกแบบโครงสร้างเชิงประกอบแบบรังผึ้งพร้อมคุณสมบัติทางการดัดงอที่โดดเด่นสำหรับการใช้งานในอุตสาหกรรมและในโครงสร้างที่หลากหลาย

สาขาวิชา วิศวกรรมเครื่องกล

ลายมือชื่อนิสิต

.....

ปี 2564

ลายมือชื่อ อ.ที่ปรึกษาหลัก

การศึกษา

.....

# # 6370108121 : MAJOR MECHANICAL ENGINEERING

KEYWORD: Sandwich Beam, Honeycomb Core, Bending, Lightweight Structure

Dechawat Wannarong : ELASTIC BENDING BEHAVIOUR OF SANDWICH COMPOSITE STRUCTURES WITH ABS CORES BY USING ADDITIVE MANUFACTURING. Advisor: Assoc. Prof. THANYARAT SINGHANART, Ph.D.

Maintaining the lightweight performance of sandwich structures while achieving good bending strength and stiffness is difficult. Core materials for these programmable sandwich constructions are 3D printed with hexagonal honeycomb, re-entrant honeycomb, and circular honeycomb topologies with varying core densities. The bending stiffness and strength of these sandwich structures are determined by a three points bending test including an Acrylonitrile Butadiene Styrene core and a unidirectional carbon fibre reinforced polymer face sheet. The sandwich composite with the greater relative core density displays greater bending strength and stiffness than the composite with the lower relative core density. The sandwich composites beam with re-entrant honeycomb core exhibit the strongest bending strength and stiffness due to negative Poisson's ratio. The findings were compared with experimental data using finite element analysis. Experiments and finite element analysis reveal that designed core structures can be used to regulate bending qualities. These results provide fresh light on the design of sandwich composite structures with exceptional mechanical characteristics for a broad variety of industrial and structural applications.

Field of Study: Mechanical Engineering

Student's Signature

.....

Academic Year: 2021

Advisor's Signature

.....

## ACKNOWLEDGEMENTS

After two years, this study has finally reached its conclusion. So many individuals have contributed to this accomplishment. Firstly, I am thankful to my advisor, Associate Professor Thanyarat Singhanart, who braved a challenging duty by walking beside me during the duration of my thesis study. I appreciate you listening to me every week and guiding me.

Secondly, my technician, Nisit Saiyalak, has been extremely helpful in teaching me how to use the universal testing machine and addressing any concerns I have had about the experiment.

Thirdly, I am grateful to Associate. Professor. Gridsada Phanomchoeng and Associate. Professor. Jirapong Kasivitanuay for agreeing to serve on this thesis committee, and to Dr. Sedthawatt Sucharitpwatskul for agreeing to serve as an external examiner of this thesis in order to provide feedback and guidance.

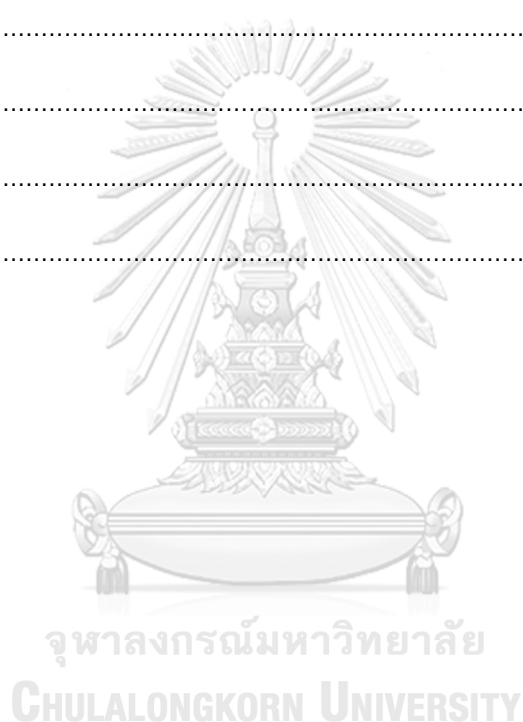
Lastly, I would want to thank my family and everyone who supported me psychologically or physically over these years of research for their contributions to this success.

## TABLE OF CONTENTS

	Page
ABSTRACT (THAI) .....	iii
ABSTRACT (ENGLISH) .....	iv
ACKNOWLEDGEMENTS .....	v
TABLE OF CONTENTS .....	vi
LIST OF TABLES .....	viii
LIST OF FIGURES .....	ix
CHAPTER 1 INTRODUCTION .....	1
1.1 Background and Rationale .....	1
1.2 Objectives of Research .....	2
1.3 Expected Benefits .....	3
1.4 Outline .....	3
CHAPTER 2 REVIEW OF EXISTING LITERATURE .....	4
CHAPTER 3 RELATED THEORY .....	8
CHAPTER 4 METHODOLOGY .....	10
4.1 Materials .....	10
4.2 Honeycomb Core Cell Design .....	11
4.3 Specimens Preparation .....	14
4.3.1 Preparation of Tensile Test Specimens .....	15
4.3.2 Preparation of Three-point Bending Test Specimens .....	17
4.3.3 Specimens Inspection .....	18
4.4 Tensile Test .....	19



4.5 Three Points Bending Test.....	20
4.6 Modelling and Meshing of Sandwich Honeycomb Structure .....	23
CHAPTER 5 RESULTS AND DISCUSSION .....	27
CHAPTER 6 CONCLUSIONS .....	41
6.1 Research Conclusions .....	41
6.2 Recommendation for Future Works .....	41
REFERENCES.....	43
APPENDIX A .....	47
APPENDIX B .....	48
VITA .....	49



## LIST OF TABLES

	Page
Table 1 Design parameter of hexagonal, re-entrant and circular honeycomb (unit mm). .....	12
Table 2 Parameters of tensile test specimen of carbon fibre reinforced polymers. ....	16
Table 3 Parameters of tensile test specimen of Acrylonitrile Butadiene Styrene. ....	17
Table 4 Parameters of the three-points bending test specimens (unit in mm.) ....	18
Table 5 Three points bending test specimen inspection including the mass, parallel and thickness.....	19
Table 6 The tensile properties of acrylonitrile butadiene styrene.....	20
Table 7 The tensile properties of unidirectional carbon fibre reinforced polymer. ....	20
Table 8 Parameters of the bending test loading device (unit in mm.) ....	21
Table 9 Peak load, bending strength, and bending stiffness obtained for each scenario of sandwich beam with honeycomb core. ....	33
Table 10 The bending stiffness between the experiment and finite element analysis and maximum load from finite element analysis. ....	35

## LIST OF FIGURES

	Page
Figure 1 The deformation of the sandwich structure .....	4
Figure 2 (a) Three-point bending and (b) Cross section A-A.....	9
Figure 3 Unidirectional carbon fibre reinforced polymer plate. ....	11
Figure 4 The schematic of three lattice structures (a) hexagonal honeycomb, (b) re-entrant honeycomb, and (c) circular honeycomb. ....	12
Figure 5 Printed hexagonal honeycomb core at relative density of 0.3 .....	13
Figure 6 Printed hexagonal honeycomb core at relative density of 0.5 .....	13
Figure 7 Printed re-entrant honeycomb core at relative density of 0.3 .....	13
Figure 8 Printed re-entrant honeycomb core at relative density of 0.5 .....	14
Figure 9 Printed circular honeycomb core at relative density of 0.3.....	14
Figure 10 Printed circular honeycomb core at relative density of 0.5.....	14
Figure 11 Tensile test specimen according to ASTM D3039 (unit in mm.). ....	15
Figure 12 Tensile test specimen according to ASTM D3039 (unit in mm). ....	15
Figure 13 Carbon fibre reinforced polymer tensile test specimen. ....	16
Figure 14 Tensile test specimen according to ASTM D638. ....	16
Figure 15 The schematic of the sandwich beam.....	18
Figure 16 The sandwich composite beam with hexagonal core at relative density of 0.5 .....	18
Figure 17 Three-point bending device. ....	21
Figure 18 The partition device on three-point bending test. ....	22
Figure 19 The specimen is fixed at the specify span length. ....	22

Figure 20 The indenter is attached along the specimen. ....	22
Figure 21 The assembling of sandwich honeycomb with carbon fibre plate and rollers. .....	23
Figure 22 The top face sheet was split into three bodies. ....	25
Figure 23 The bottom face sheet was split into five bodies. ....	25
Figure 24 The meshing of the sandwich honeycomb structure. ....	26
Figure 25 The meshing of the honeycomb core. ....	26
Figure 26 The meshing at the centre of the sandwich honeycomb. ....	26
Figure 27 Load-deflection curves of sandwich beam with re-entrant honeycomb core at relative density of 0.3 and 0.5. ....	28
Figure 28 Load-deflection curves of sandwich beam with hexagonal honeycomb core at relative density of 0.3 and 0.5. ....	28
Figure 29 Load-deflection curves of sandwich beam with circular honeycomb core at relative density of 0.3 and 0.5. ....	29
Figure 30 Load-deflection curves of sandwich beam with hexagonal, re-entrant, and circular honeycomb core at relative density of 0.3. ....	29
Figure 31 Load-deflection curves of sandwich beam with hexagonal, re-entrant, and circular honeycomb core at relative density of 0.5. ....	29
Figure 32 The deflection of the sandwich beam during the stage 2. ....	30
Figure 33(left) Enlarged picture of core failure morphology of hexagonal core. ....	31
Figure 34(right) Enlarged picture of core failure morphology of re-entrant core. ....	31
Figure 35 Enlarged picture of core failure morphology of circular core. ....	31
Figure 36 The maximum Von-Mises stress at the hexagonal honeycomb core. ....	32
Figure 37 The maximum Von-Mises stress at the re-entrant honeycomb core. ....	32

Figure 38 The maximum Von-Mises stress at the circular honeycomb core. ....	33
Figure 39. The bending stiffness between the experiment and finite element analysis. ....	35
Figure 40 The maximum load between the experiment and finite element analysis. ....	35
Figure 41 (a,b) Enlarged picture of printed circular honeycomb core at relative density of 0.3 and 0.5, respectively. ....	39
Figure 42 (a,b) Enlarged picture of printed re-entrant honeycomb core at relative density of 0.3 and 0.5, respectively. ....	39
Figure 43 (a,b) Enlarged picture of printed hexagonal honeycomb core at relative density of 0.3 and 0.5, respectively. ....	40



# CHAPTER 1

## INTRODUCTION

This chapter introduces the background and rationale of this research. In addition, the objectives and expected benefits are also informed in this chapter. Consequently, the thesis outline is discussed in this chapter.

### 1.1 Background and Rationale

Sandwich composite structures are rapidly being employed in a wide range of technical applications such as automotive, aerospace, satellite applications, marine vessels, and others. A structure is typically made up of three substructures. The outermost layer is a thin layer that attempts to evenly disperse burst pressure throughout the second and third substructure, referred to as the bonding layer and core, respectively. Sandwich structures have several properties that make them appealing for engineering applications. This includes stiffness and strength with a high mass specific stiffness for light weighting. Among the many forms of core structure, honeycomb designs offer the benefit of increasing bending stiffness and buckling resistance. A vast number of experiments have been carried out in order to understand the complexity of core designs and topologies. Meanwhile, recent advances in additive printing process allow for greater flexibility in both designing and constructing honeycomb structures with complicated core shapes. Furthermore, there is a significant need for lightweight parts in technical applications such as the automobile sector and others. Lightweight alternative materials, such as aluminium, magnesium alloy, and composite materials, are being used in particular to decrease the weight and enhance the rigidity of sandwich structures now made with conventional materials. Carbon fibre reinforced polymer, a typical lightweight material with particular strength and stiffness superior to metals, is regarded as the materials to replace traditional metals.

The materials employed in the building of a sandwich structure, the core topology, and the geometry of the face layer all have an impact on its mechanical performance. Nonetheless, despite their technological benefits, sandwich architectures

are now being held back by a variety of problems. These include comparative assessment, which is important at the moment since potential specifiers of sandwich materials frequently lack the expertise and experience needed to adequately analyse their net advantages. In addition, novel methods to sandwich structure design and production are being investigated. The efficient deployment of sandwich structures frequently necessitates the development of novel design techniques. This might involve novel insights on the product concepts as well as non-traditional manufacturing techniques. A vast number of experiments have been carried out in order to understand the complexity of core designs and topologies. However, there is a scarcity of data on the bending behaviour of sandwich constructions with honeycomb cores composed of the thermoplastic materials acrylonitrile butadiene styrene. The effect of sandwich core geometric arrangement on bending behaviour is unknown. Tough service conditions are becoming increasingly prevalent, resulting in a wider range of damage hazards under diverse pressures such as axial compression, localized impact, and bending. When subjected to bending loads, the bending strength and stiffness of sandwich constructions must be investigated further. To use these materials in a variety of applications, knowing their bending behaviour is a crucial, as is a deeper comprehension of the various failure processes underneath static loading circumstances. Consequently, the goals of this study were to examine the bending behaviour of sandwich constructions with varied relative core densities and core topologies, including hexagonal honeycomb, re-entrant honeycomb, and circular honeycomb. The honeycomb core materials are acrylonitrile butadiene styrene, which was manufactured using additive manufacturing process, and the face sheet material is unidirectional carbon fibre reinforced polymer. The experiment's results are compared using finite element analysis.

## 1.2 Objectives of Research

- To design the three distinct core topologies with the use of additive manufacturing.

- To analyse the bending stiffness of sandwich structures with various core relative densities and core topologies by using finite element analysis.
- To experimentally investigate the tensile characteristics of materials and three-point bending behaviour of sandwich structure.
- To verify the bending behaviour from the finite element analysis by comparing with the experiment.

### 1.3 Expected Benefits

Sandwich composite structures are increasingly being used in a variety of technological applications, including automotive, aerospace, satellite applications, marine vessels, and others. Studying the bending behaviour of sandwich composite structures with varied honeycomb structures might offer a better knowledge of sandwich structure deflection under various applied loads. Acrylonitrile butadiene styrene is used to create the honeycomb structure. The face sheet is composed of unidirectional carbon fibre reinforced polymer. This information may be applied and enhanced in a variety of technical applications.

### 1.4 Outline

This thesis, excluding the introduction, was organised into four chapters. Chapter 2 discusses the results of a review of sandwich composite structures and additive manufacturing. Chapter 3 discusses the related theory of bending behaviour. Chapter 4 describes the technique, which includes the materials utilised, the design of honeycomb core cell, the preparation of tensile test specimens, the preparation of bending test specimens, the experiment, and the modelling and meshing of sandwich composite construction. In Chapter 5, the findings and discussion of this investigation are discussed. The conclusion of this study and recommendation for future works are presented in Chapter 6.



## CHAPTER 2

### REVIEW OF EXISTING LITERATURE

Sandwich structures are presently widely used as low weight materials in the airplane, automotive, and civil engineering sectors due to their excellent bending stiffness and energy absorption characteristics [1]. A structure is typically made up of three substructures. As illustrated in Figure 1, the outermost layer is made up of a thin layer that seeks to disperse burst pressure more equally across the second and third substructures known as the bending layer and core, respectively. Several studies have found that component material, geometrical parameters, and core cell design all have a substantial on mechanical performance [2, 3]. Sandwich constructions were often exposed to bending forces in engineering applications. As a consequence, bending performance tests, including failure load, deflection, and failure mechanism, are critical in practical applications [4].

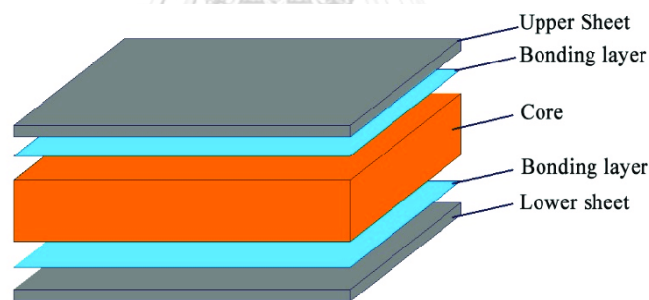


*Figure 1 The deformation of the sandwich structure [5].*

Additive manufacturing is becoming increasingly popular for both research and industry applications. The phrase added substance refers to the fact that, rather than removing information to frame a section as is done in traditional technique. One of the advantages of 3D printing was the ability to create intricate components and products in combinations that would otherwise be unattainable [6]. Acrylonitrile Butadiene Styrene (ABS) and Polylactic Acid (PLA) are the most often used materials in 3D printing. Saad and Sabah [7] examined the mechanical properties of acrylonitrile butadiene styrene and polylactic acid produced using fused deposition modelling, a type of additive manufacturing technique. The design consists of a core design that increases the

proportion of infill by increasing the volume of hexagonal pores. Tensile strength and modulus were shown to increase considerably with increasing packing density. The increase in tensile strength and bending stiffness is due to an increase in the number of honeycomb cores, and as the cross-sectional area rises, so does the resistance to applied pressures [7]. Compared to other thermoplastics, acrylonitrile butadiene styrene has higher resistance to bending and elongation before breaking. Polylactic acid is praised for its flexibility, while acrylonitrile butadiene styrene is praised for its toughness [8]. Furthermore, the tensile and flexural characteristics of blended materials, as well as conventional ABS and PLA, were assessed using ASTM D638 for tensile testing and ASTM D790-17 for flexural testing. Specimens composed of 80 percent PLA and 20 percent ABS showed higher tensile strength than other specimens, according to the findings. Despite the fact that samples created at lower feed rates were preferable because the structure of the polymer microfibrils was clearer and more uniform, the overall strength was enhanced. However, when 100 percent ABS and 100 percent PLA are taken into account. In terms of flexural strength and elongation before breaking, acrylonitrile butadiene styrene (ABS) beat polylactic acid (PLA) [9]. This result is consistent with the patterns observed in conventional materials by Blok et al. [8]. Furthermore, the mechanical characteristics of 3D printed materials are affected by layer thickness and cross section form. Wan, Lin, and Hu's study found that ABS printed with a thickness layer of 0.254 mm had higher tensile strength than samples printed with a thickness layer of 0.330 mm [10]. These findings are similar with those of Tymrak, Kreiger, and Pearce, who studied the tensile strength of ABS and PLA at different deposition layer thickness [11].

In particular, alternative lightweight materials such as aluminium, composite materials, and magnesium alloy are being used in engineering applications to reduce the weight and enhance the rigidity of the final product. Carbon fibre reinforced polymers, a product that will ultimately substitute the conventional metals in the construction industry is believed to be a typical light material with greater toughness and strength than metals. A prepreg fabric structure and stacking sequences are often

responsible for determining the mechanical characteristics of carbon fibre reinforced polymer products consisting of bending rigidity and tensile strength, as well as other qualities [12-14]. The majority of these research have solely looked at the mechanical properties of carbon fibre reinforced polymer plates, which includes their bending behaviour when subjected to a variety of stacking angles. Therefore, more study is required in addition to enable the evaluation of the mechanical characteristics of carbon fibre reinforced polymers in sandwich structures to be carried out.

Honeycomb structures have seen greater application because to the growing need for lightweight and performance-based materials in the structural domain. Auxetic materials, also known as negative Poisson's ratio materials, are a unique family of mechanical metamaterials that exhibit the odd property of getting thicker when expanded [15]. The unit cell's geometric configuration and the mechanical properties of the core fabric may be used to define the straight elastic behaviour of typical honeycombs [16]. Numerous studies have been carried out to determine the effect of a negative Poisson's ratio on the mechanical properties of honeycomb cores. Li et al. [17] investigated the mechanical properties of honeycomb cores with a negative Poisson's ratio, which included a chiral truss and a re-entrant honeycomb, in order to better understand their behaviour. When compared to the non-negative Poisson's ratio, which comprised a honeycomb and a truss, this set of cores performs better. It has been demonstrated that auxetic lattice reinforced composites outperform non-auxetic lattice reinforced composites in terms of mechanical performance, providing a unique mix of energy absorption and rigidity. On the other hand, Miller et al. [18] investigated the mechanical properties of a honeycomb core with chiral structure. The data indicated that the structures had a negative Poisson's ratio, which corroborated Li et al. [17]. The major criteria determining flexure characteristics, according to prior study, are sheet thickness, honeycomb height, and honeycomb orientation [5]. Sandwich cores constructed of Nomex paper honeycombs are the most effective. These lightweight cores have poor compressive and shear properties, which causes them to deflect significantly. Although these sandwich structures are generally built of conventional

thermoset or metallic mixed incompatible materials, they provide a recycling problem because they are not recyclable. Recyclable thermoplastic materials are becoming increasingly common in modern engineering applications as a means of addressing this problem. Gao et al. [19] developed fully thermoplastic honeycomb sandwich structures made of continuous glass fibre reinforced polypropylene face sheets, a polypropylene core, and a thermoplastic film assembly. Meanwhile, the ply sequence and the thickness of the face sheet had the largest impact on the failure modes, which were mostly Li and Ma in incidence [5, 19]. According to certain research, the sandwich beam's bending characteristics are influenced by the core topologies. It may be quite difficult to create a sandwich construction that is both lightweight and strong. However, data on the bending behaviour of sandwich structures with different honeycomb core architectures made of the thermoplastic materials acrylonitrile butadiene styrene are few. It is uncertain what influence the geometric layout of the sandwich core has on the bending behaviour.

Additionally, finite element analysis may be utilized to perform bending analysis on sandwich honeycomb structures. ANSYS software is used to create models and meshed. Because the face sheets were meshed with a regular rectangular form, the SHELL 91 element type was employed [20]. Another study found that quadrilateral mesh elements were preferred over the triangular mesh elements because the aspect ratio of a quadrilateral can be controlled close to one [21]. Three-point bending tests were used to validate the finite element model using typical honeycomb sandwich panels. The two techniques revealed that the deformation behaviours were quite comparable and displayed the same patterns of local indentation [19, 22]. Thus, when simulating the honeycomb core design of a sandwich beam, the finite element model can be regarded as an appropriate technique.

### CHAPTER 3

#### RELATED THEORY

Bending stiffness is a property that indicates how well it resists deformation in response to an applied force. The stiffness,  $k$ , is defined as shown below.

$$k = \frac{P}{\delta} \quad (1)$$

The parameter  $P$  signify the applied force and  $\delta$  denoted the member's deformation in the direction of the applied force.

For sandwich beam in three-point bending, the elastic analysis is outlined here. Suppose a sandwich beam of span  $L$  and width  $W$  loaded in three points bending with a central load  $P$  as depicted in Figure 2(a) and 2(b). Because of the interplay between material qualities and geometric dimensions, the bending properties of sandwich structures are highly dependent on their construction.  $D$ , the equivalent bending stiffness of a sandwich beam, was explored in order to better understanding its bending properties. It is assumed that the skins stay securely attached to the core, the beams cylindrically with no curvature in the  $yz$  plane, and that cross sections remain parallel to the beam's longitudinal axis [23, 24]. As a result,  $D$  is simplify obtained as shown in Equation (2).

$$D = D^1 + D^2 = \frac{E_f W f^3}{6} + \frac{E_f W f d^2}{2} + \frac{E_c W h^3}{12} \quad (2)$$

The bending stiffness is comprised of two components, as shown in Equation (2). The first is the face sheets contribution. Sandwich core is responsible for the second contribution.  $E_f$  and  $E_c$  signify the face sheet's and sandwich core's elastic modulus, respectively.

Bending strength is critical for evaluating the bending behaviour of sandwich beams, since this directly influences the products service life. Calculation of bending strength,  $\sigma_s$ , may be conducted using the simplified beam model [25]. Bending strength was determined as follows.

$$\sigma_s = \frac{3P_m L_s}{2WH^2} \quad (3)$$

The parameter  $P_m$  denoted the maximum load in three points bending and  $L_s$  denotes the span distance.

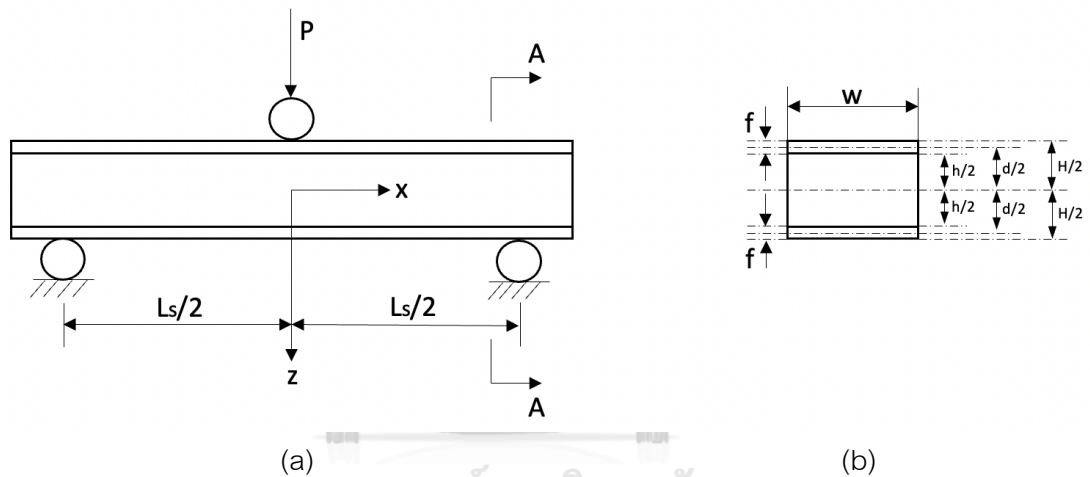


Figure 2 (a) Three-point bending and (b) Cross section A-A

## CHAPTER 4

### METHODOLOGY

This chapter describes the materials used in the building of sandwich honeycomb constructions. Also discussed in this chapter is the fundamental design of honeycomb core cell. In terms of content, the samples preparation was divided into three major categories: the production of tensile test specimens, the preparation of three-point bending test specimens, and the inspection of the specimens. In addition, the process for performing tensile and three-point bending tests using a universal testing machine is provided. This chapter ends with a discussion of sandwich honeycomb structure modelling and meshing.

#### 4.1 Materials

The unidirectional carbon fibre reinforced polymer plate is provided by XC Carbon Fibre Co.,Ltd. (Guangdong, China), and the thickness of the plate is one millimetre as shown in Figure 3. The unidirectional carbon fibre reinforced polymer plate is processed by hot press one layer by one layer which consist of 0.2 millimetres for each ply of carbon fibre cloth T300 with the total of 5 plies. This type of carbon fibre reinforced polymer plate is employed as a portion of the sandwich structure's face sheet. The honeycomb core structure is made up of Acrylonitrile Butadiene Styrene (ABS). Additive manufacturing is used by Harn Engineering Solutions Public Company Limited, located in Bangkok, Thailand, in order to print acrylonitrile butadiene styrene in the shape of various honeycomb structures. These structures will be examined in further detail in section 4.2. Using the method of melting extrusion modelling, the printing machine has the capacity to print a maximum volume of up to 20 centimetres on each of its three dimensions. Epoxy resin is used in the construction of the glue that is known as RS PRO Adhesive. This two-part rapid-setting epoxy comes in two individual tubes and may be applied to a wide range of surfaces. This particular form of epoxy glue has a setting time of three hours at room temperature and a gel time of four to six minutes, allowing the material to be adjusted into the desired position with perfect accuracy.

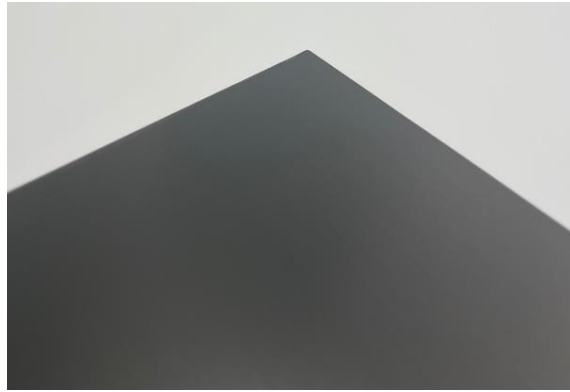


Figure 3 Unidirectional carbon fibre reinforced polymer plate.

#### 4.2 Honeycomb Core Cell Design

The geometric aspects of the planned sandwich design philosophy of hexagonal honeycomb, re-entrant honeycomb, and circular honeycomb are addressed in this section. The schematic of three lattice microstructures is shown in Figure 4(a), 4(b) and 4(c), respectively. A honeycomb's relative density ( $\rho^*/\rho_s$ ), where  $\rho^*$  is the density of honeycomb and  $\rho_s$  is the density of honeycomb when it is full solid. Each configuration's relative density can be determined as follows:

For hexagonal honeycomb

$$\frac{\rho^*}{\rho_s} = \frac{(t/L)[(H/L) + 2]}{2\cos\theta[(H/L) + \sin\theta]} \quad (4)$$

For re-entrant honeycomb

$$\frac{\rho^*}{\rho_s} = \frac{(t/L)[(H/L) + 2]}{2\cos\theta[(H/L) + \sin\theta]} \quad (5)$$

For circular honeycomb

$$\frac{\rho^*}{\rho_s} = \frac{(T/R)[1 - (T/2R)]\pi}{\sqrt{3}} \quad (6)$$



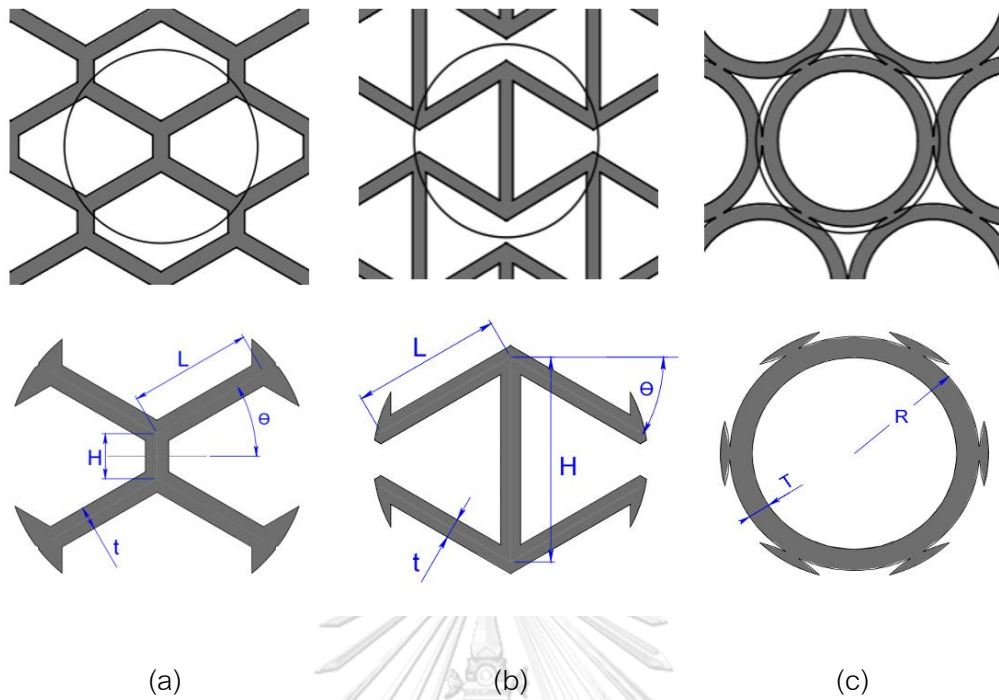


Figure 4 The schematic of three lattice structures (a) hexagonal honeycomb, (b) re-entrant honeycomb, and (c) circular honeycomb.

In this study, relative densities of 0.3 and 0.5 are taken into account. The relative density can be varied by altering the thickness of the cell wall of each honeycomb structure, while three types of cellular structures are configured to have the same unit cell dimension of 16 mm x 16 mm. As a consequence, the thickness of cell walls in each arrangement may be determined using Equation (4), (5) and (6). Table 1 details the parameters for each lattice structures.

Table 1 Design parameter of hexagonal, re-entrant and circular honeycomb (unit mm).

$\frac{\rho^*}{\rho_s}$	Hexagonal Honeycombs				Re-entrant Honeycombs				Circular Honeycombs	
	$L$	$H$	$t$	$\theta$	$L$	$H$	$t$	$\theta$	$T$	$R$
0.3	9.24	3.38	1.76	30°	9.24	12.62	1.23	30°	1.45	8
0.5	9.24	3.38	2.92	30°	9.24	12.62	2.06	30°	2.64	8

After designing the honeycomb core, the honeycomb was manufactured using additive manufacturing. Using fused deposition modelling 3D printing, a build platform is moved by an extrusion nozzle as it travels horizontally and vertically. To build a three-dimensional item, thermoplastic material is heated to a high temperature and then extruded. The filaments are extruded layer by layer with a diameter of 0.4 mm. The honeycomb sized 75 mm in width, 200 mm in length, and 10 mm in thickness. Figure 5 to Figure 10 demonstrate the honeycomb cores that were printed with different core topologies, including hexagonal, re-entry, and circular honeycomb.

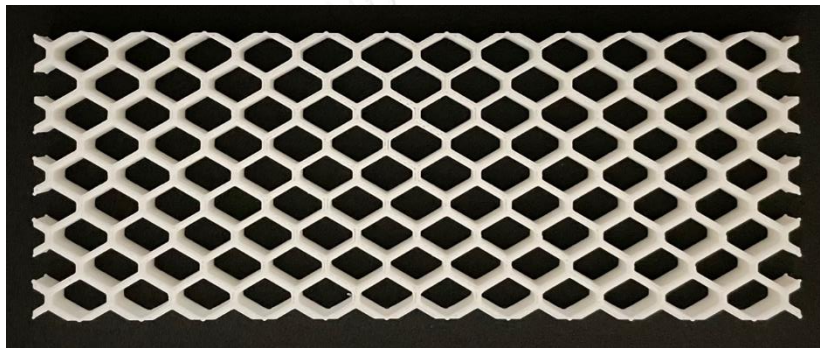


*Figure 5 Printed hexagonal honeycomb core at relative density of 0.3*

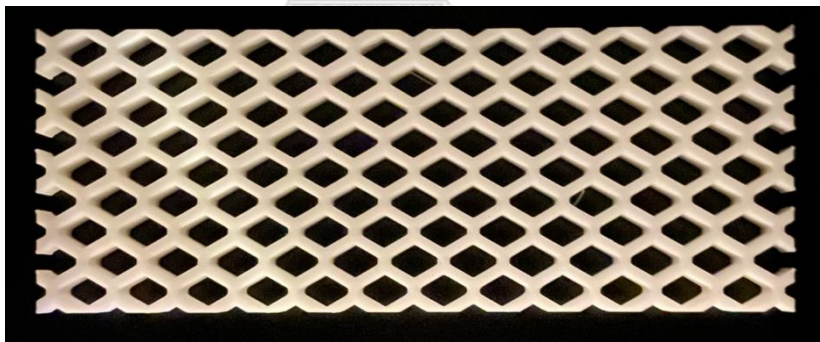


*Figure 6 Printed hexagonal honeycomb core at relative density of 0.5*

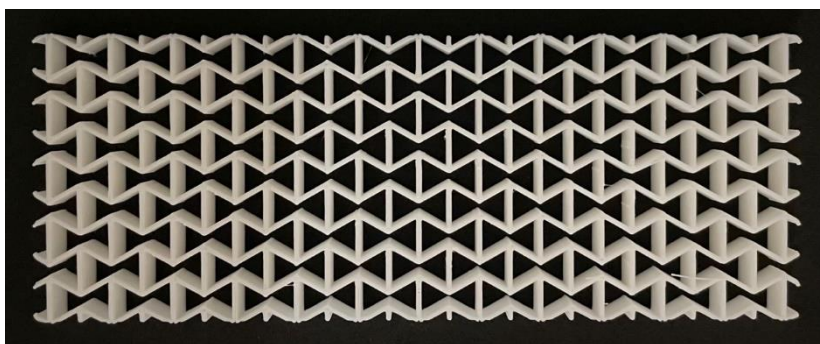


*Figure 7 Printed re-entrant honeycomb core at relative density of 0.3*

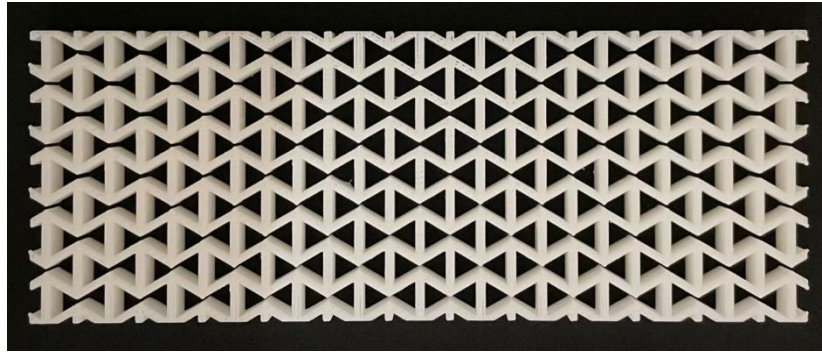


*Figure 8 Printed re-entrant honeycomb core at relative density of 0.5*

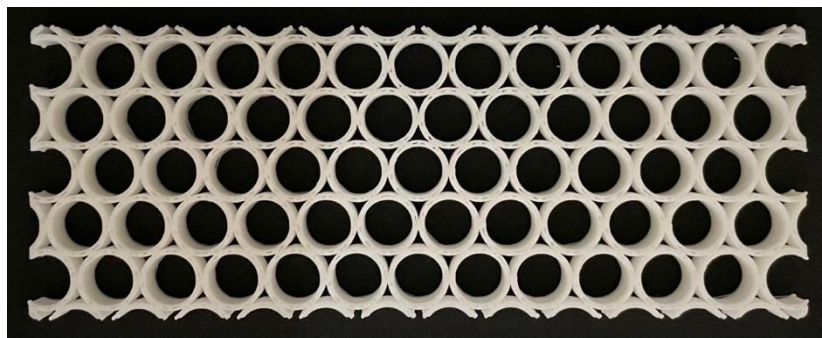


*Figure 9 Printed circular honeycomb core at relative density of 0.3*

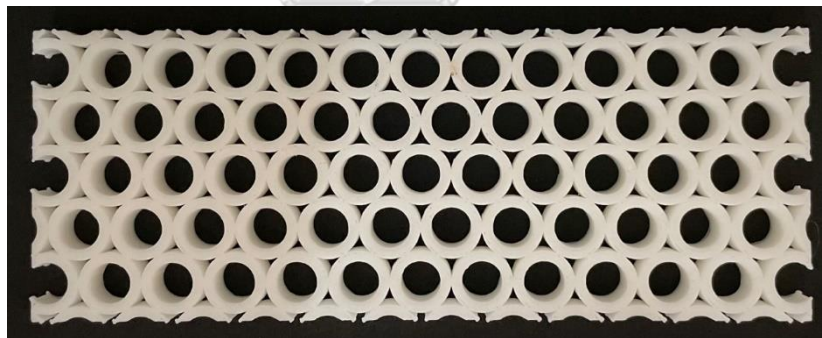


*Figure 10 Printed circular honeycomb core at relative density of 0.5*

### 4.3 Specimens Preparation

In sections 4.3.1 and 4.3.2, the preparation of the tensile test specimens and three-point bending test specimens is described in detail. In addition, samples were inspected after the production of the specimen, which will be explained in depth in section 4.3.3.

#### 4.3.1 Preparation of Tensile Test Specimens

The mechanical characteristics of the cured unidirectional carbon fibre reinforced polymer plates were acquired by tensile testing in order to perform strength analysis of the carbon fibre reinforced polymer product. Tensile specimens with dimensions of 250 mm x 25 mm were made in the 0°, 45°, and 90° direction in accordance with ASTM D3039 [26]. The biaxial extensometer is used to measure the Poisson's ratio. Figure 11 and Figure 12 depict the dimension schematic for carbon fibre reinforced polymer tensile test specimens. Moreover, aluminium tabs were added to either side of the specimens to avoid breakage due to applied pressure of the hydraulic grips. Table 2 shows the parameters of tensile test specimen of unidirectional carbon fibre reinforced polymers. U is short for the unidirectional carbon fibre reinforced polymer. The number following U is stand for the fibre direction. As the original size of the unidirectional carbon fibre reinforced polymer plate was 500 mm by 500 mm, a waterjet was used to cut the plate to the dimensions listed in Table 2. Waterjet cutting had the benefit of preventing dust containment. A waterjet blows all carbon dust into the water tank, where it is easier to manage and dispose of. Figure 13 depicts the unidirectional carbon fibre-reinforced polymer tensile test specimen that was affixed with an aluminium tab and prepared for tensile testing.

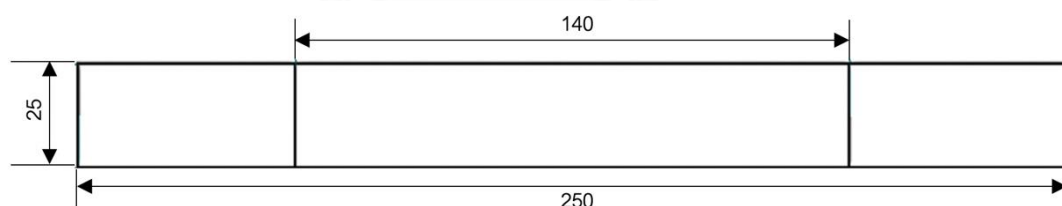


Figure 11 Tensile test specimen according to ASTM D3039 (unit in mm.).

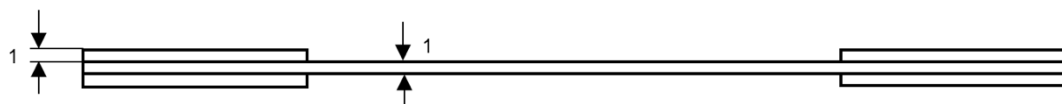


Figure 12 Tensile test specimen according to ASTM D3039 (unit in mm.).



Table 2 Parameters of tensile test specimen of carbon fibre reinforced polymers.

Type	Panel Size W x L (mm)	Fibre Direction	Number
U0	25 x 250	0°	3
U45	25 x 250	45°	3
U90	25 x 250	90°	3



Figure 13 Carbon fibre reinforced polymer tensile test specimen.

The material characteristics of Acrylonitrile Butadiene Styrene (ABS) are determined by uniaxial tensile testing in accordance with the ASTM D638 [27] standard. A waterjet machine is used to cut ABS sheet with a thickness of 2 mm into a dog-bone shape. Flat specimens are often machined into a dog-bone form to ensure that the break happens in the centre of the specimen rather than at clamping region. The geometry of the dog-bone type IV tensile test is depicted in Figure 14. The parameters of tensile test specimen of Acrylonitrile Butadiene Styrene are shown in Table 3.

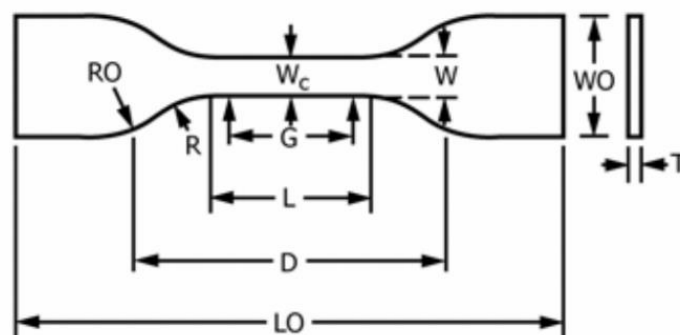


Figure 14 Tensile test specimen according to ASTM D638.

*Table 3 Parameters of tensile test specimen of Acrylonitrile Butadiene Styrene.*

Type	Dimension (mm)		Number
ABS	W	6	3
	L	33	
	WO	19	
	LO	115	
	G	25	
	D	65	
	R	14	
	RO	25	
	T	2	

#### 4.3.2 Preparation of Three-point Bending Test Specimens

The bending test specimens are manufactured according to ASTM C393 [28] standard. The sandwich beams are designed to have overall dimensions of 200 mm x 75 mm x 12 mm. The schematic of the sandwich beam is shown in Figure 15. Table 4 shown the parameters of the three points bending test specimen. H is short for hexagonal honeycomb, R is short for re-entrant honeycomb, and C is short for circular honeycomb. The number followed H, R, and C mean the relative core density of the core where number 1 stand for the relative core density at 0.3 and 2 stand for the relative core density at 0.5. U stand for unidirectional carbon fibre reinforced polymer plate. For instance, H2U means the sandwich beam with hexagonal honeycomb core with relative core density at 0.5 and unidirectional carbon fibre reinforced polymer face sheets. The unidirectional carbon fibre reinforced polymer plate was cut using the waterjet. Now after all the face sheets and core material have been completed, epoxy resin is used to join two face sheets to one core structure at room temperature by applying the pressure. All specimens are maintained attached for one day to ensure that they are adhesively linked, then dried for three days to enables cohesion between the face sheets and the core. The sandwich composite beam was cleaned to eliminate the influence of leftover epoxy on the three point bending test, including the surfaces and the sides of the

sandwich composite beam. Figure 16 depicts the sandwich composite beam specimen that ready for the three-point bending test.

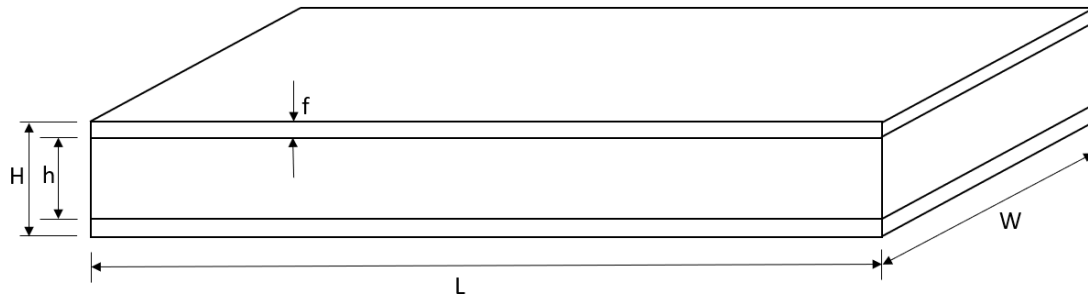


Figure 15 The schematic of the sandwich beam.

Table 4 Parameters of the three-points bending test specimens (unit in mm.)

Length, L	Width, W	Face Sheet Thickness, f	Core Thickness, h	Total Thickness (without bonded layer), H
200	75	1	10	12



Figure 16 The sandwich composite beam with hexagonal core at relative density of

0.5

#### 4.3.3 Specimens Inspection

Prior to printing, the mass of the honeycomb core was calculated using the programme. The relative core density of 0.3, based on the design of the core, should weigh 76 grammes. Despite having a relative density of 0.5, the core should have weighed 112 grammes. After the honeycomb cores were printed, they were weighed by using the digital scale to ascertain their actual mass. Table 5 contains the values of the specimens. It is evident that the masses of all cores were almost identical to the design.

All cores that are 3D printed must be flat and parallel. This is established by putting the core on the levelled table, ensuring there is no space between the table and the core and measuring the thickness. The U-CFRP plate was weighed by using the digital scale to ascertain their actual mass which is 3 grammes. After applying epoxy to adhere the core to the face sheet, the weight of the sandwich beam was measured for checking excessive amount of epoxy inside the core. In addition, the sandwich beams' thickness was measured at six positions by using digital vernier calliper and the average thickness was determined as shown in Table 5. According to the patterns shown in Table 4, the thickness of the specimen without bonded layer was 12 mm. However, the non-uniform thickness of the epoxy layer will affect the standard deviation of the specimen.

*Table 5 Three points bending test specimen inspection including the mass, parallel and thickness.*

Sample	Core Mass (g)	Core Parallel and Flat	Sandwich Beam Thickness (mm)	Beam Thickness (Standard Deviation)	Sandwich Beam Mass (g)
H1U	75.80	Yes	12.68	0.04	97.51
H2U	112.13	Yes	12.78	0.07	123.52
R1U	76.10	Yes	12.39	0.06	97.22
R2U	111.93	Yes	12.56	0.03	125.64
C1U	75.73	Yes	12.81	0.03	103.87
C2U	111.43	Yes	12.63	0.11	132.36

#### 4.4 Tensile Test

The loading programme for the tensile test on carbon fibre reinforced polymers and acrylonitrile butadiene styrene is carried out in accordance with the American Society for Testing and Materials' standard test protocol so that the material properties can be precisely identified, and the data can be used in finite element analysis. Tensile testing in accordance with ASTM D3039 is used to ascertain the amount of force



required to fracture a polymer composite specimen as well as the degree to which the specimen stretches or lengthens up until it breaks. The ASTM D3039 standard specimens are subjected to a specified test speed of 2 mm/min. To compute tensile modulus and extension, an extensometer or strain gauge is needed. The tensile test may determine the elastic modulus in fibre direction (E11) using sample U0, elastic modulus in transverse direction (E22) using sample U90, shear modulus in 1-2 plane (G12) using sample U45, and Poisson's ratio (V12) using sample U0. Tensile testing with acrylonitrile butadiene styrene was also performed in line with the ASTM D638 standard. It is accomplished by applying a tensile force to a dog-bone specimen and observing the specimen's various properties under stress. The specimen is tensile tested at a rate of 2 mm/min until it fails. Young's modulus, Poisson's ratio, tensile yield strength, and tensile ultimate strength are all calculated. The tensile properties of materials are shown in Table 6 and Table 7.

*Table 6 The tensile properties of acrylonitrile butadiene styrene.*

Materials	Young's Modulus (MPa)	Poisson's Ratio	Tensile Yield Strength (MPa)	Tensile Ultimate Strength (Pa)
ABS	2390±36.05	0.399±0.07	44.1±1.96	44.3±1.72

*Table 7 The tensile properties of unidirectional carbon fibre reinforced polymer.*

Property	Value	Unit
Elastic modulus in fibre direction	56.3±4.05	GPa
Elastic modulus in transverse direction	8.81±2.24	GPa
Shear modulus in 1-2 plane	7.15±1.15	GPa
Poisson's ratio	0.20±0.05	

#### 4.5 Three Points Bending Test

The bending test uses the electronic universal testing machine. The type is Autograph AG-IS 100 KN with a maximum loading force of 100 KN. The loading program corresponds to American Society for Testing and Materials which are ASTM

C393 standard test technique for flexural characteristics of sandwich structures. The test principle is to evaluate the force-deflection of the sandwich construction using the beam three-point bending test. A 150 mm support span with the centre loading is used in the three-point flexure test. The diameter of the indenter and the support were 25 mm. The bending specimen is placed in the middle of the upper indenter and the below supports, which are both steel cylinders. Figure 17 depicts a three-point bending device, and Table 8 depicts the loading device's specification. In addition, to ensure that the specimen is in the correct position, the partition is constructed to secure the specimen in equal dimensions, as seen in Figure 18 and Figure 19. After the specimen has been secured, the universal testing machine's zero point is adjusted, and the load is delivered vertically to the centre of the specimen. During this process, the gap between the test indenter and the specimen has also been assessed to confirm that the indenter is attached along with the specimen and there is no space between the specimen and the indenter as shown in Figure 20. The test indenter's loading rate is 6 mm/min, and the sampling rate was every 0.25 seconds. The test is conducted until the maximum load has dropped and the load has stabilised. After the test was done, the bending stiffness and strength can be determined by using Equation (1) and (3).

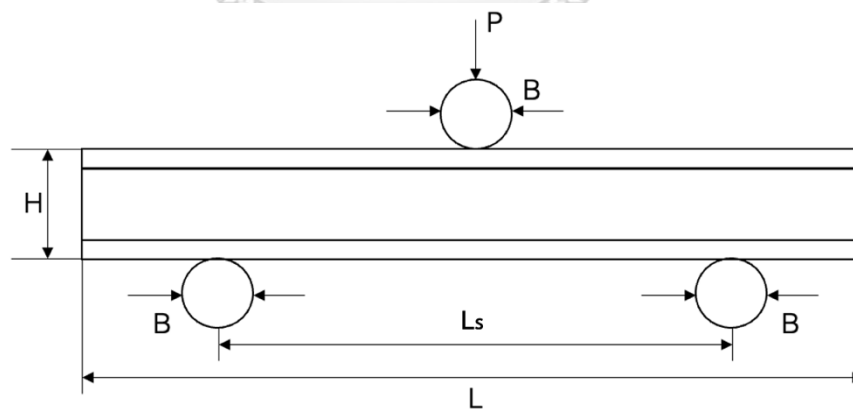


Figure 17 Three-point bending device.

Table 8 Parameters of the bending test loading device (unit in mm.)

Span, $L_s$	Diameter of indenter and support, $B$	Length, $L$	Height, $H$
150	25	200	12



*Figure 18 The partition device on three-point bending test.*



*Figure 19 The specimen is fixed at the specify span length.*

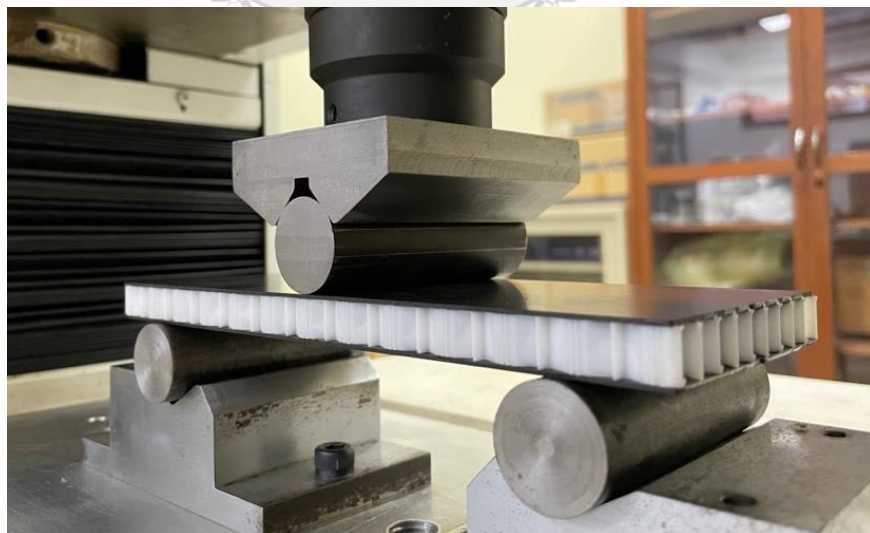


*Figure 20 The indenter is attached along the specimen.*

#### 4.6 Modelling and Meshing of Sandwich Honeycomb Structure

Finite element analysis was used to analyse the honeycomb sandwich construction. It is mechanical engineering simulation software that may be used to analyse any engineering problem that requires a computational solution. A finite element analysis tool is used to discover solutions for structural components in linear and nonlinear investigations, as well as hydrodynamic and explicit research. A finite element issue is expressed as a partial differential equation, the solution to which is achieved by adding boundary conditions. Prior to finite element analysis, the core, face sheets, and rollers were created by using the Solidworks, and meshing of the model were done in ANSYS software.

Solidworks is used to produce the core, face sheets, and rollers, which are comprised of six components: a core, two face sheets, and three rollers, as shown in Figure 21. These six components are being assembled.

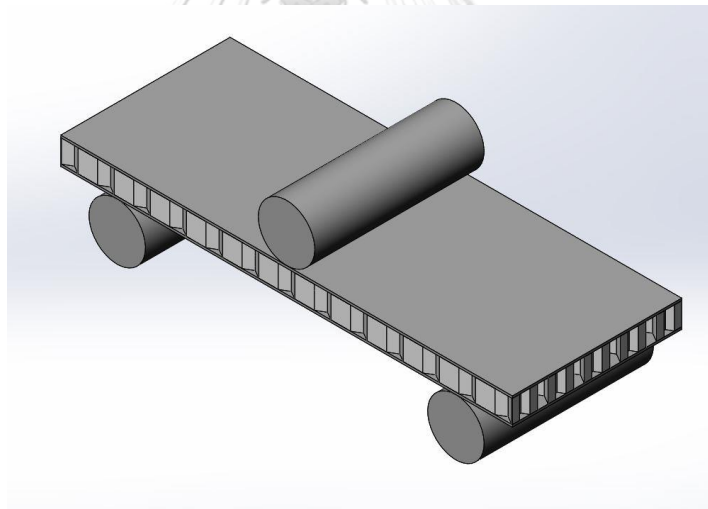


*Figure 21 The assembling of sandwich honeycomb with carbon fibre plate and rollers.*

The layer of epoxy is neglected in this finite element analysis because of the layer of epoxy is too thin compared to other elements. In addition, in order to evaluate the bending behaviour of honeycomb sandwich constructions using finite element analysis, the engineering data is used to identify the material characteristics of acrylonitrile butadiene styrene and unidirectional carbon fibre reinforced polymer. This is completed so that the honeycomb sandwich constructions can be evaluated for their

ability to bend. The tensile tests of each material that were carried out in accordance with ASTM D3039 and ASTM D638 provided the foundation for the engineering data that is used for the analysis. The material characteristics of acrylonitrile butadiene and unidirectional carbon fibre reinforced polymer are detailed in Tables 6 and 7, respectively. In order to facilitate the process of simply separating the mesh zone, the top face sheet was split into three bodies, and the bottom face sheet was split into five bodies as shown in Figure 22 and Figure 23, respectively. Additionally, the frictional connections were determined to be the contacts that were made between the rollers and the face sheets. Bonded was chosen as the kind of connection to use between the face sheets and the core. This ensures that there will be no gaps or slippage between the face sheet and the core. After the connections were allocated, the mesh convergence research was conducted as shown in Appendix A. In finite element modelling, a finer mesh often yields a more precise solution. However, when a mesh is becoming more refined, calculation time rises as the number of elements and number of nodes increases. For this, a denser element distribution is used to reconstruct the mesh, re-analyse it, and then compare the findings. The final mesh size was chosen when the findings had stabilised. Various mesh sizes were employed for different parts of this investigation. The face sheet had a body sizing of 7 mm, while the core and roller used a body sizing of 4 mm. There were four divisions for the face sheet edges and five for the core as shown in Figure 24 and Figure 25. In addition, the BIAS option was used to divide the sandwich honeycomb structure at the centre of the sandwich beam into twenty divisions so that the results would be more accurate as depicted in Figure 26. This was done because the location where the maximum deflection will occur is at the centre of the sandwich honeycomb structure. The load is applied in a vertical direction at the indenter, and the fixed support boundary condition is applied to both sides of the support's boundary condition. From the finite element analysis, it is possible to ascertain the deflection of the sandwich structure as well as the Von-Mises stress after the boundary conditions and the load have been applied.

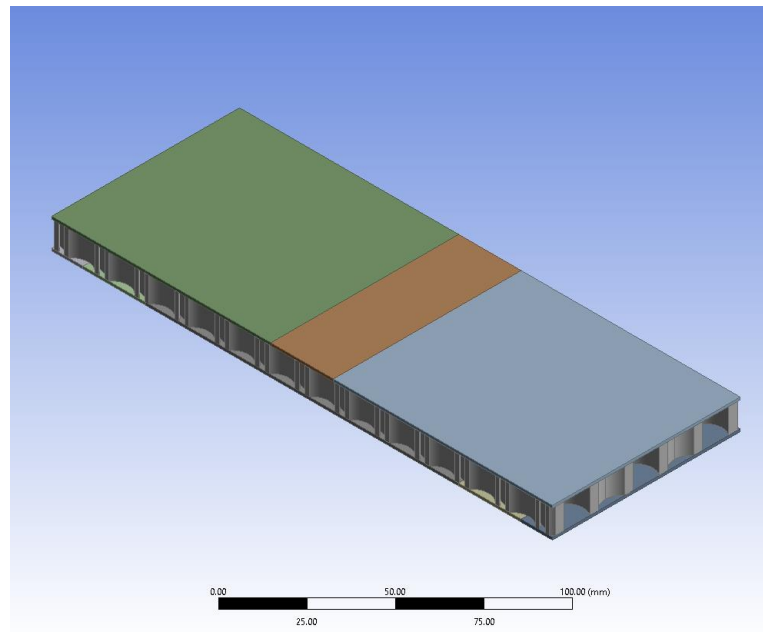


Figure 22 The top face sheet was split into three bodies.

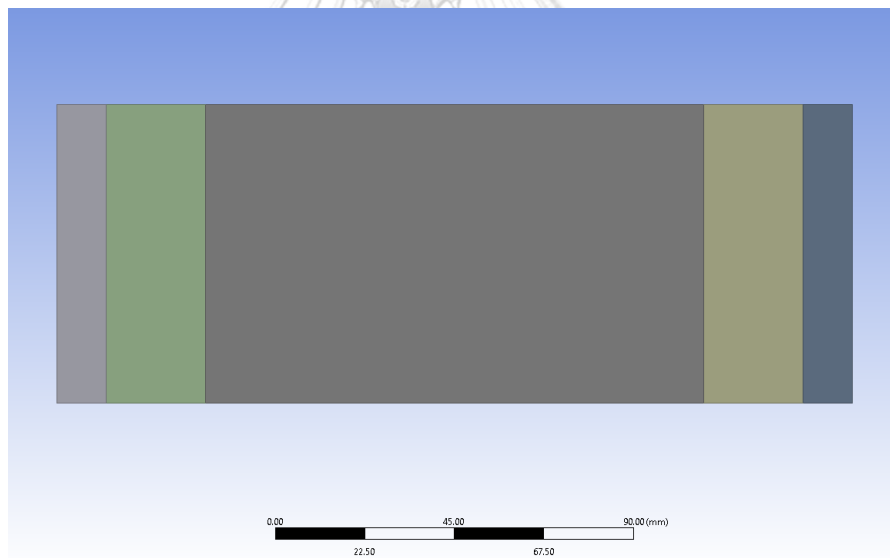


Figure 23 The bottom face sheet was split into five bodies.

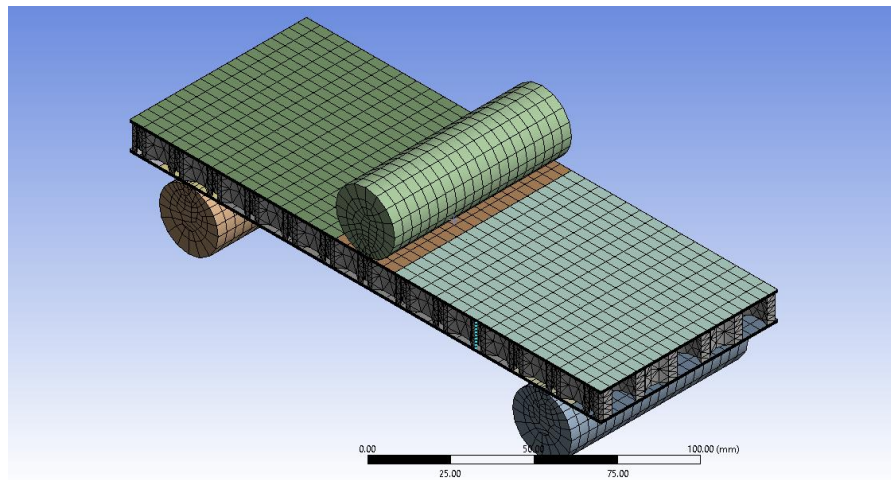


Figure 24 The meshing of the sandwich honeycomb structure.

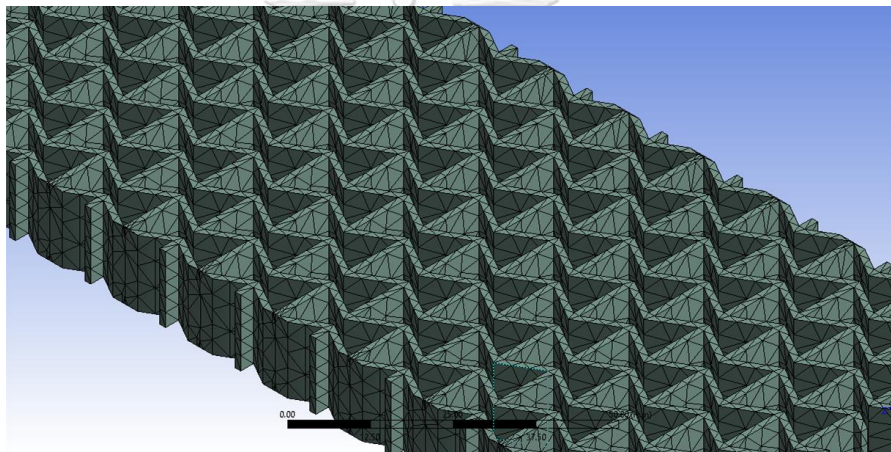


Figure 25 The meshing of the honeycomb core.

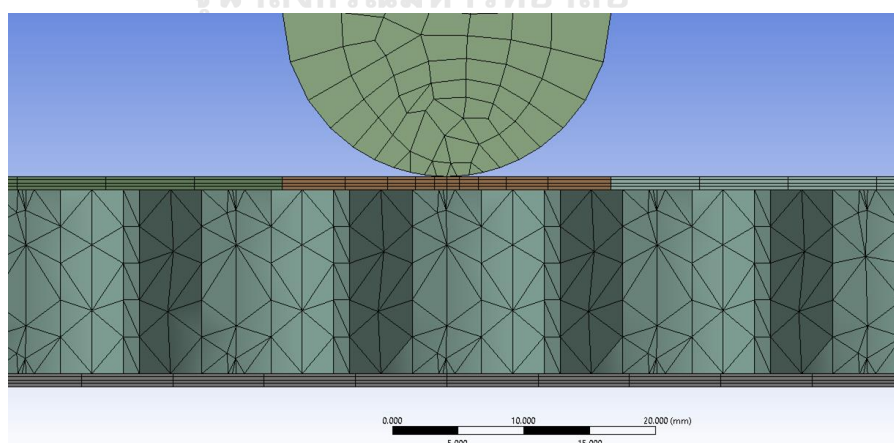


Figure 26 The meshing at the centre of the sandwich honeycomb.



## CHAPTER 5

### RESULTS AND DISCUSSION

The results of a three-point bending test were discussed in this chapter. The test was conducted on a sandwich composite honeycomb structure with a variety of core topologies and relative densities. The results included the maximum load and bending stiffness. Both the experiment and the finite element analysis were used to make a comparison about the stiffness. Additionally, this part discusses the effects of relative core density on bending strength and stiffness, and the effects of core topology on bending strength and stiffness.

Figure 27 through Figure 31 each exhibit an experimental curve for the three-point bending load-deflection relationship for a distinct architected sandwich structure, along with the face sheet and cores that corresponds to that structure. Figure 27 depicts the load-deflection curves of a sandwich beam arrangement with a re-entrant honeycomb core at relative core densities of 0.3 and 0.5. The load-deflection curves can be mainly divided into three main stages. The first stage is the linear elastic stage, the force increases linearly until reaches its peak, when yielding occurs. The second stage, after the yield point there is an abrupt decrease in load owing to local collapse. The final stage is where the load has steadied owing to the face sheet structure's load carrying and the honeycomb just acted as a linking layer. The load-deflection curves of a sandwich beam arrangement with a hexagonal honeycomb and circular honeycomb core at relative densities of 0.3 and 0.5 with unidirectional carbon fibre reinforced polymer face sheets are shown in Figure 28 and Figure 29, respectively, these sandwich beams with alternative core topologies display the same response. Loads have been seen to increase significantly with increasing relative density. The subsequent phases demonstrate the same regularity, with a considerable increase in load-bearing capacity as relative density rises, meaning that a core with a high relative density has a greater ability to resist bending forces. In addition, Figure 30 and Figure 31 illustrate the load-deflection curves of a sandwich beam with a hexagonal, re-entrant, and circular honeycomb core with a core density of 0.3 and 0.5, respectively. Figure 32 depicts the



bending behaviour of sandwich beam from three-point bending test. The deflection of the sandwich beam was measured from the displacement sensor at the indenter. The experimental results show that the re-entrant core at relative density of 0.5 has the maximum peak force among all other cores. Noticeably, hexagonal core design at relative density of 0.3 has the minimum peak force among all other cores. In addition, at the last stage of the force against deflection curve, the load did not decrease to zero owing to the face sheet structure's load carrying.

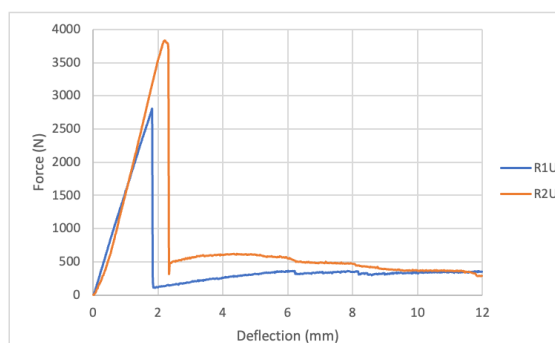


Figure 27 Load-deflection curves of sandwich beam with re-entrant honeycomb core at relative density of 0.3 and 0.5.

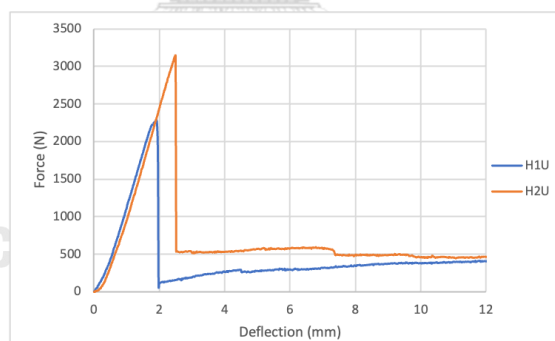


Figure 28 Load-deflection curves of sandwich beam with hexagonal honeycomb core at relative density of 0.3 and 0.5.

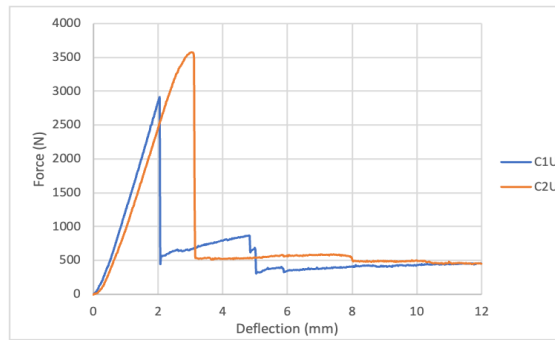


Figure 29 Load-deflection curves of sandwich beam with circular honeycomb core at relative density of 0.3 and 0.5.

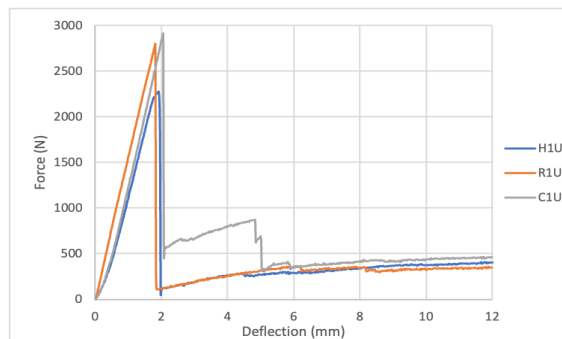


Figure 30 Load-deflection curves of sandwich beam with hexagonal, re-entrant, and circular honeycomb core at relative density of 0.3.

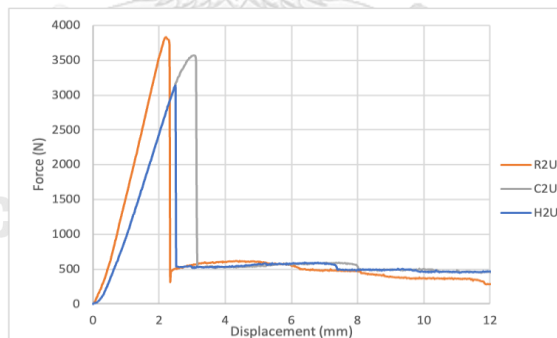
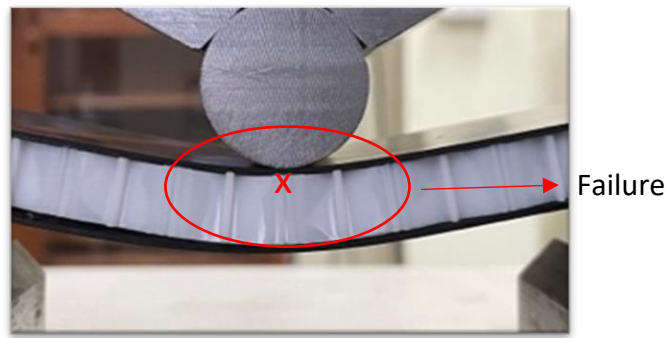


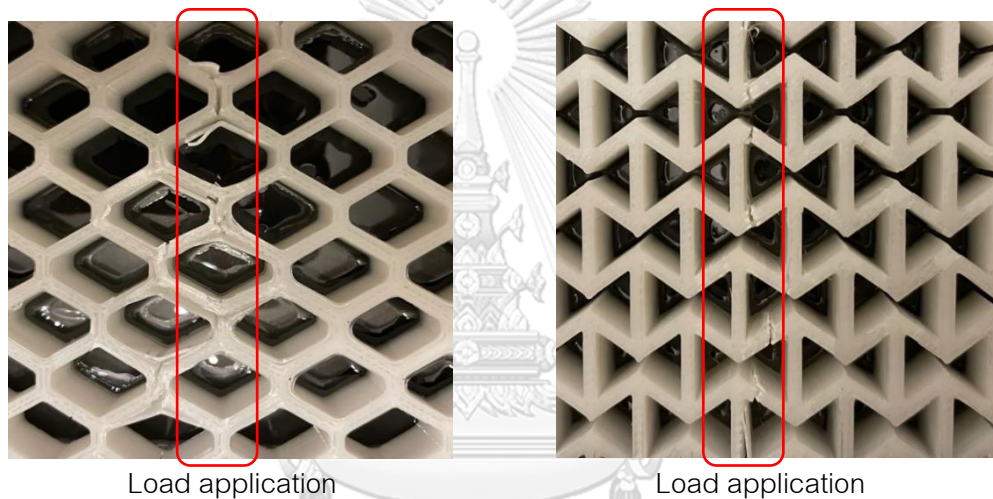
Figure 31 Load-deflection curves of sandwich beam with hexagonal, re-entrant, and circular honeycomb core at relative density of 0.5.



*Figure 32 The deflection of the sandwich beam during the stage 2.*

Sandwich constructions may fail in a variety of ways when subjected to three-point bending. The failure of the sandwich honeycomb might result from the failure of the core or the skin. When the stress in either of the skins surpasses the in-plane strength of the face sheet material, the top skin yields and fails owing to face yielding. Moreover, honeycomb sandwich architectures might break owing to core failure when loaded in bending. Under bending loads, core failure is one of the most prevalent types of failure in sandwich structures as the material properties of the core was lower than the material properties of the face sheets [29]. There are three primary failure mechanisms of sandwich honeycomb core. Face sheet tension or compression due to bending. Core shear failure and core compressive failure are examples of potential failures. Core compressive failure will dominate right below the load application line. While the shear failure of the core will dominate only next to the load application line [30]. As observing from the experiment, the failure occurs at the centre of the core where the maximum stress was occurred at the top surface of the core. To observe the failure, the top face sheet was removed from the core, since there is a small delamination between the top face sheet and the core. During the three-point bending test, the hexagonal honeycomb core failed, as shown in Figure 33. Figure 34 shows the core failure of the re-entrant honeycomb core, and Figure 35 shows the core failure of the honeycomb core in a circular shape. Core fractures happen in the hexagonal, re-entrant, and circular honeycomb sandwich composite constructions. These core fractures are also obvious from the decreases in the load-deflection curves, which shows that these sandwich structures would collapse locally. There is a good agreement between the experiment

and finite element analysis that the core will fracture at the top surface of the core and at the mid span of the honeycomb core as shown in Figures 36, 37 and 38. It is clear that all the honeycomb cores in this study had a core compressive failure, as the failure was occurred at the midspan and was just below the load application line, and it was caused by the yield stress of the core's material. Furthermore, the failure of the circular honeycomb seems to have happened between the unit cell connections and was parallel to the printed filament as shown in the arrowhead in Figure 38. In addition, the breakdown of the hexagonal honeycomb core occurred when the yield stress of the core's material was equivalent to the yield stress of the parallel-printed filament material.

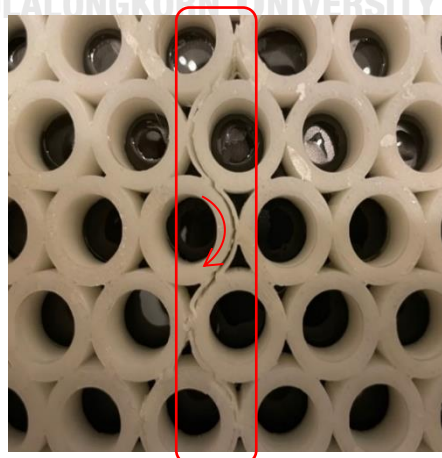


Load application

Load application

Figure 33(left) Enlarged picture of core failure morphology of hexagonal core.

Figure 34(right) Enlarged picture of core failure morphology of re-entrant core.



Load application

Figure 35 Enlarged picture of core failure morphology of circular core.

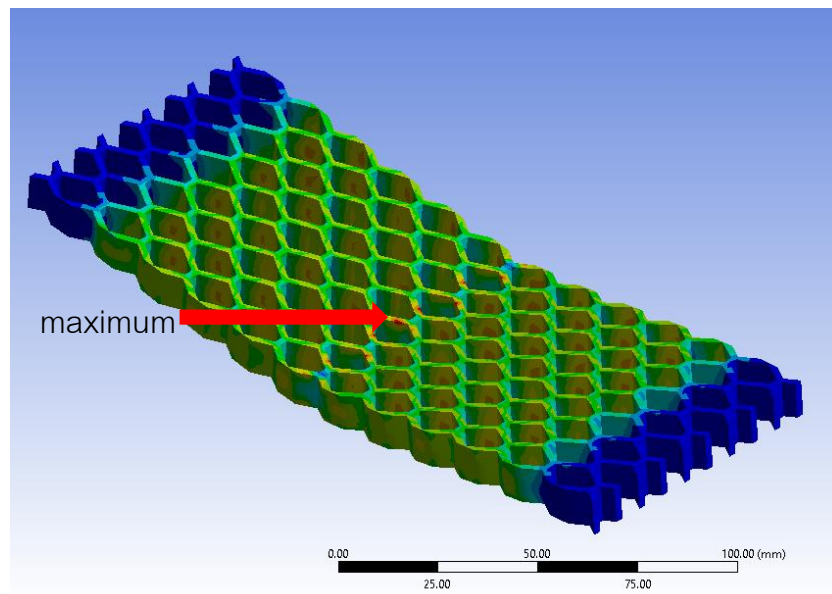


Figure 36 The maximum Von-Mises stress at the hexagonal honeycomb core.

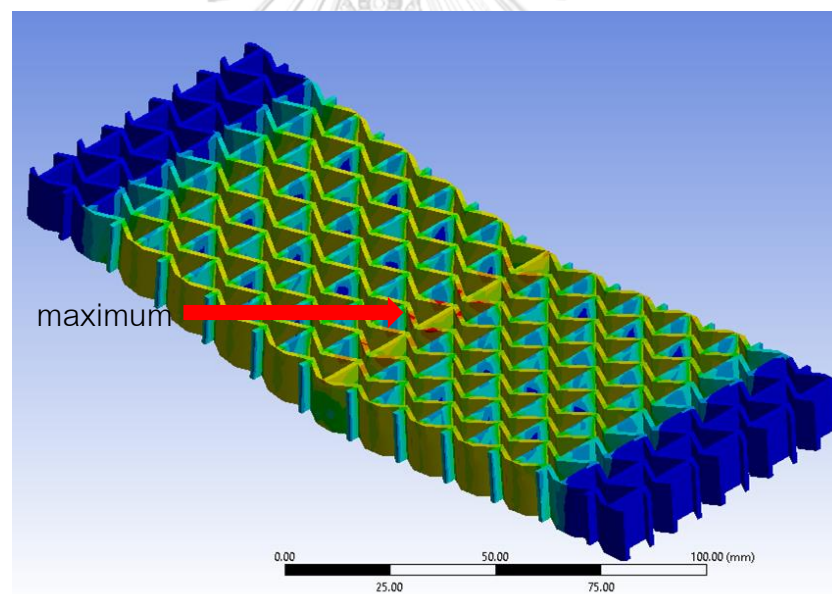


Figure 37 The maximum Von-Mises stress at the re-entrant honeycomb core.

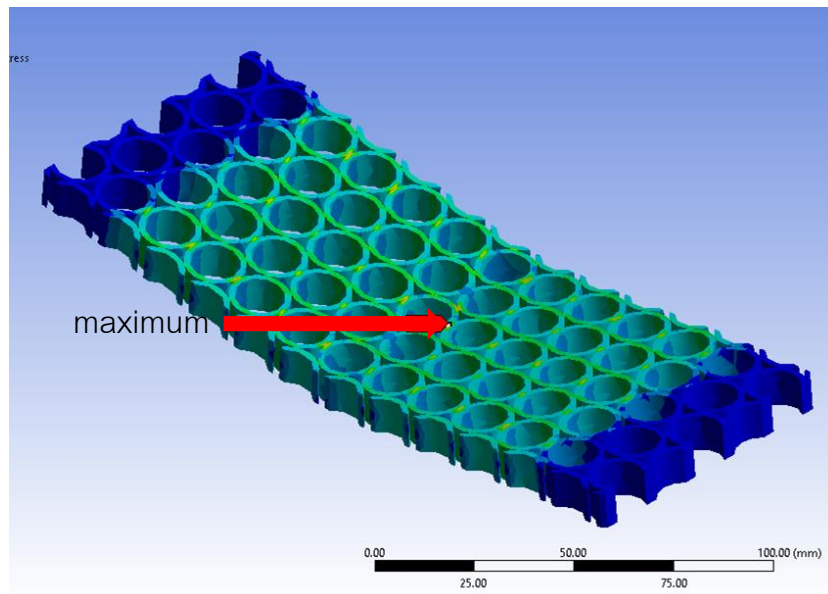


Figure 38 The maximum Von-Mises stress at the circular honeycomb core.

The bending behaviour of these sandwich beams was analysed by using Equation (1) to determine the bending stiffness and Equation (3) to determine the bending strength to get a better knowledge of the mechanical advantages of sandwich composite honeycomb cores with diverse core topologies in resisting bending. The bending strength and stiffness of each type of specimen can be determined as shown in Table 9.

Table 9 Peak load, bending strength, and bending stiffness obtained for each scenario of sandwich beam with honeycomb core.

Core Topology	Core Relative Density	Configuration		
		$P_m$ (N)	$\sigma_s$ (MPa)	$k$ (N/mm)
Hexagonal	0.3	2281 $\pm$ 32.01	47.5	1464 $\pm$ 21.42
	0.5	3142 $\pm$ 25.41	65.4	1497 $\pm$ 18.57
Re-entrant	0.3	2800 $\pm$ 29.15	58.3	1524 $\pm$ 23.46
	0.5	3840 $\pm$ 19.58	80	2022 $\pm$ 24.71
Circular	0.3	2912 $\pm$ 38.74	60.6	1572 $\pm$ 42.15
	0.5*	3571 $\pm$ 41.10	74.4	1484 $\pm$ 39.78

Note: \*invalid (further details will be discussed in the following section)

In order to determine the sandwich construction's bending stiffness using finite element analysis, a variety of bending loads were applied to the structure and analysed from the slope of the force vs deflection graph. Table 10 displays the bending stiffness calculated from the finite element analysis as well as the results of the experiment. When the findings of a finite element analysis are compared to the data that was collected through experiments, it will become clear that the numerical results and the experimental results are in the same trend regarding the fact that the bending stiffness increased as the relative core density increased. In addition, the maximum load was determined from the results of the finite element analysis by applying the maximum Von-Mises criterion to the honeycomb core by comparing with the tensile yield strength of the acrylonitrile butadiene styrene material that obtained from the tensile test, more details are shown in Appendix B. Von-Mises is mostly used to ductile materials. The material will yield if the Von-Mises stress of the material under load is equal to or higher than the yield strength of the same material. According to the findings, there is a discrepancy in the calculated value of the maximum load between the experimental data and the results of the finite element analysis as shown in Figure 40. Moreover, it is noticeable that the re-entrant honeycomb structure at a relative density of 0.5 can resist a higher bending load, whereas the hexagonal honeycomb core at a relative density of 0.3 can resist the lowest bending load, which was in agreement with the experiment. This finding was made possible by the honeycomb's hexagonal shape. However, the maximum load of both re-entrant and circular honeycomb differs significantly between experiment and finite element analysis. The impact of the experimental error on the finite element analysis will be examined in later section.



Table 10 The bending stiffness between the experiment and finite element analysis and maximum load from finite element analysis.

Core Topology	Core Relative Density	$k(\text{N/mm})$			$P_m(\text{N})$		
		Experiment	FEA	% diff.	Experiment	FEA	% diff.
Hexagonal	0.3	1464	1767	17%	2281	3589	32%
	0.5	1497	2089	28%	3142	3600	10%
Re-entrant	0.3	1524	1933	21%	2800	7237	61%
	0.5	2022	2281	11%	3840	9500	60%
Circular	0.3	1572	1875	16%	2912	6200	53%
	0.5	1484	2187	32%	3571	8850	60%

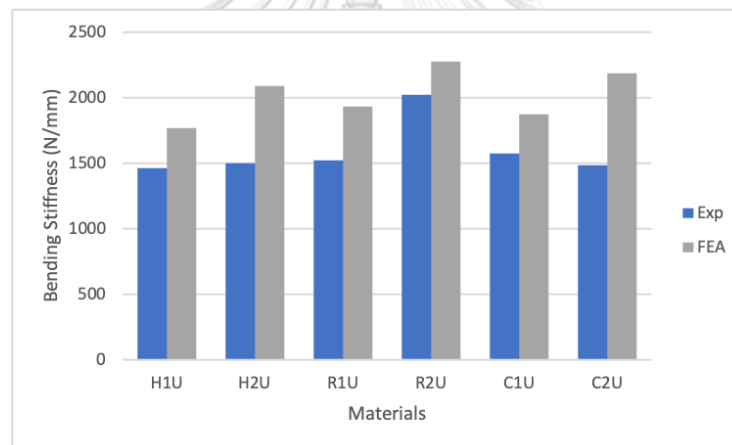


Figure 39. The bending stiffness between the experiment and finite element analysis.

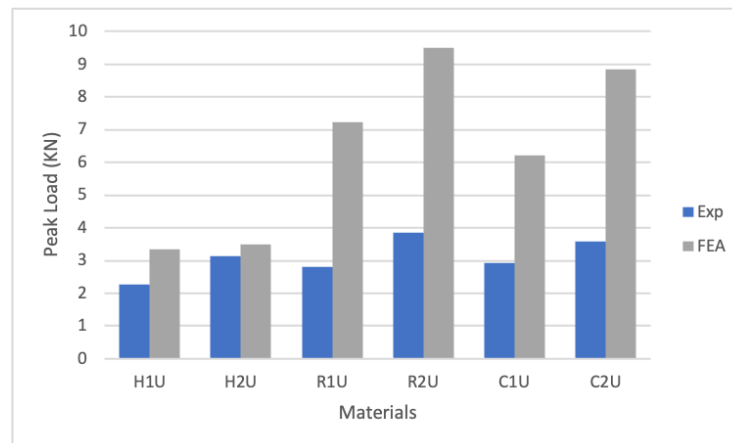


Figure 40 The maximum load between the experiment and finite element analysis.



The core structure and relative density of the core were compared in the cases of re-entrant honeycomb, hexagonal honeycomb, and circular honeycomb. Each scenario takes the core density at 0.3 and 0.5 into account. Taking into account the impact of core density on bending strength, as the relative core density increased so did the bending strength increased, as seen in Table 9. By increasing the relative core density from 0.3 to 0.5, the bending strength of both hexagonal and re-entrant honeycomb was raised by about 37%. Moreover, the bending strength of circular honeycomb was raised by about 22%. The greater relative core density indicates that the structure of the cell wall is more densely packed, resulting in an increase in the unit cell's surface area. As the surface area increases, the stress distribution along the sandwich core structure will changed. Additionally, the maximum stress will be reduced when the relative core density increased. The finite element analysis clearly shown that the stresses in the honeycomb core at lower relative core density are greater than those at higher relative core density. For example, the stress of the re-entry honeycomb core at a relative density of 0.3 was 3.21 MPa, whereas the stress at a relative density of 0.5 was 3.10 MPa. This behaviour gives the structure a greater ability to withstand greater loads. Therefore, in order to design the strength of the sandwich panel, a higher relative core density can resist a larger bending strength.

In addition, take into account the influence of core topology on bending strength. For all three fundamental honeycomb topologies, including hexagonal, re-entrant, and circular. The hexagonal honeycomb has the lowest bending strength of all relative core densities, as is evident. While the re-entrant has the highest bending strength value followed by the circular honeycomb. This is because the re-entrant structure has a negative Poisson's ratio. As a result of negative Poisson's ratio, structures shifted closer together. The level of stress at the same applied bending load was lower than other structures which allowing them to withstand more bending resistance. This characteristic enables the re-entrant structure to withstand greater bending loads. During bending deformation, the hexagonal and circular structures behave differently than the re-entrant structure, suggesting a positive Poisson's ratio. However, the

bending strength of the circular honeycomb structure was found to be more than that of the hexagonal honeycomb structure. This indicates that in order to design the core topology, the negative Poisson's ratio structure is better than the positive Poisson's ratio structure.

Consider also the impact of core density on bending stiffness. The bending stiffness from the experiment of re-entrant was enhanced by 32%, while the bending stiffness of hexagonal was increased by 2.2%. This implies that the structure with larger relative core density can resist more bending stiffness. In contrast, the bending stiffness of the circular at a relative density of 0.5 was reduced by 5% compared to its bending stiffness at a relative density of 0.3. According to Equation (2), the bending stiffness of a material with a higher relative density should be greater than that of a material with a lower relative density because the relative core density increases, the elastic core modulus also increases. However, this peculiar behaviour of bending stiffness for circular honeycomb at relative density of 0.5 might be the error of the specimen's manufacturing procedure. The circular sandwich beam with a relative density of 0.5 was not properly bonded between the face sheet and the core, as shown by the thickness standard deviation value in Table 5. The thickness of the sandwich beam was not equal for all the positions of the sandwich beam. This indicates that the bending stiffness of circular sandwich honeycomb with a relative density of 0.5 was invalid. Additionally, an excessive amount of epoxy was used to produce the circular sandwich honeycomb, which was heavier than other samples. This higher amount of epoxy allows the structure to withstand the increased bending load, resulting in an increase in bending stiffness. However, the excessive mass of epoxy is small when compared with core's mass, this effect can be neglected. Therefore, in order to design the stiffness of the sandwich panel, a higher relative core density can resist a larger bending stiffness.

In order to evaluate the influence of core topologies on bending stiffness, the moment of inertia of the re-entrant and circular structures was larger than that of the hexagonal structure. Moments of inertia for re-entrant, circular, and hexagonal structures were 22111, 24203, and 21896, respectively. In addition, the influence of a negative

Poisson's ratio on a re-entrant structure may contribute to the structure's superior bending stiffness. However, the bending stiffness of the circular topology was somewhat greater than that of the re-entrant topology as a result of the extra quantity of epoxy used to maintain the structure against bending loads. As a consequence, finite element analysis reveals that the bending stiffness of the re-entrant honeycomb topology tends to be greater than that of other topologies. Then came the circular and hexagonal topologies, respectively.

In this work, it was observed that the experimental and finite element analyses have certain errors. The inaccuracy may have resulted from the procedure of creating the specimen via fused deposition modelling or during apply the load via three-point bending test. During the three-point bending test, however, the load indenter was verified to be connected and aligned with the specimen, therefore this may be disregarded as an error. Consequently, the mistake may have been caused by the printing of the core. As shown in Table 1, the thickness of the cell wall was rather thin, particularly in comparison to the thickness of the cell wall of circular honeycomb structures. Layer by layer, filaments having a diameter of 0.4 mm are extruded. For a 1 mm thick specimen, the nozzle will run about 2 times. The resolution of FDM printers is determined by the nozzle size and the accuracy of the extrude motions. Other variables also impact the accuracy and smoothness of the printed models, such as the fact that the bonding between layers is less than in SLA printing. As demonstrated in the larger image of the printed honeycomb core, there may be some space and porosity between the layer of extruded filaments in the specimen whose thickness was very thin. This is one of the limitations of fused deposition modelling-based 3D printing, which was distinct from resin-based 3D printing. Stereolithography Apparatus (SLA) printers regularly generate things with a better resolution and more accuracy than fused deposition modelling printers, however SLA printers are more costly. Figures 41(a) and 41(b) exhibit an enlarged image of a circular honeycomb core that has been produced by 3D printing. Figures 42(a) and 42(b) exhibit a magnified image of a printed re-entrant honeycomb core. Both printed circular and re-entrant honeycomb at relative densities of

0.3 and 0.5 shown a gap between the printed layers. Figures 43(a) and 43(b) exhibit a magnified image of the printed hexagonal honeycomb core. The printed hexagonal honeycomb at relative densities of 0.3 and 0.5 shown the completely printed layer.

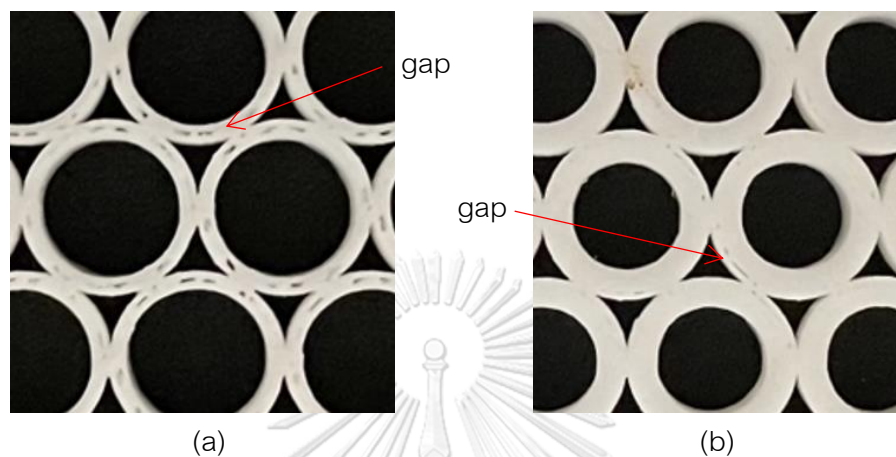


Figure 41 (a,b) Enlarged picture of printed circular honeycomb core at relative density of 0.3 and 0.5, respectively.

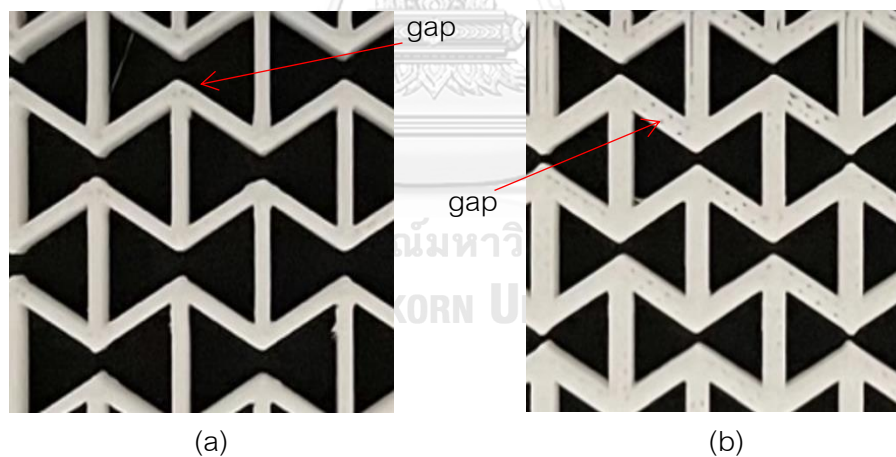
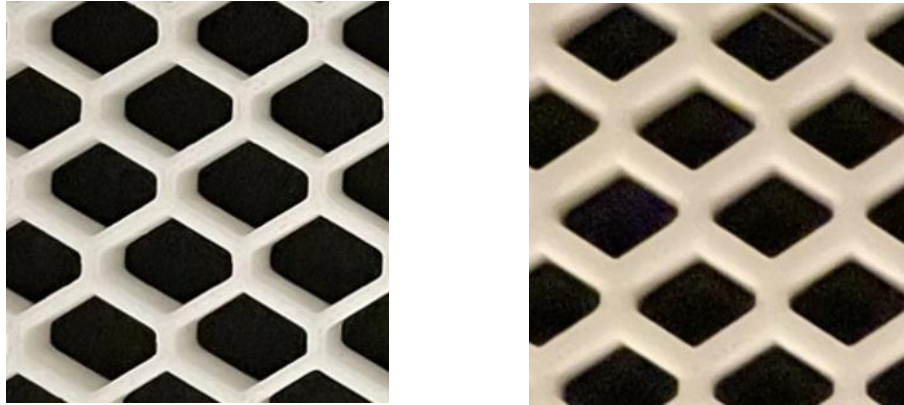


Figure 42 (a,b) Enlarged picture of printed re-entrant honeycomb core at relative density of 0.3 and 0.5, respectively.



*Figure 43 (a,b) Enlarged picture of printed hexagonal honeycomb core at relative density of 0.3 and 0.5, respectively.*

The printed circular honeycomb core for both relative core densities and the re-entrant honeycomb core for both relative densities contain a gap between each layer's bonding. This may have an effect on the core's strength, since there is a significant difference between the maximum load determined by experiment and the finite element calculations of both the circular and re-entrant honeycomb cores. The stress concentration will be larger than in a completely printed layer because of the gap or porosity. Due to the smoothness of the printed layer, the experimental and finite element analyses of the hexagonal honeycomb core produced slightly different maximum loads. In addition, the bonding layer was disregarded during the finite element analysis, which may have had an impact on the outcome. However, the results of the experiment and the finite element analysis were in excellent agreement. The bending rigidity will increase as the relative core density rises, and re-entrant structures are the most effective at resisting bending loads.

## CHAPTER 6

### CONCLUSIONS

In this chapter, the key findings of this study are summarised, and recommendations for relevant future research are offered. Consequently, these subjects are separated into two distinct sections of this chapter.

#### 6.1 Research Conclusions

We have produced a unique class of sandwich composite structures using 3D-printed core materials consisting of Acrylonitrile Butadiene Styrene and carbon fibre reinforced polymer face sheets. At core densities of 0.3 and 0.5, hexagonal honeycomb, re-entrant honeycomb, and circular honeycomb are proposed as core topologies. On these sandwich composite constructions, bending strength and bending stiffness are evaluated via three-point bending tests and finite element analysis. The sandwich composite beam with the greater relative core density displays greater bending strength and stiffness than the sandwich composite beam with the lesser relative core density. The re-entrant and circular honeycomb core designs have superior bending strength and stiffness compared to the hexagonal honeycomb core design. The relative core density and core topologies especially core with negative Poisson's ratio affect the bending strength and stiffness of the sandwich beam, as is evident. To build a sandwich composite beam with maximum bending stiffness and bending load capacity, the core would have a negative Poisson's ratio and a high relative core density. This study provides fresh light on the design of sandwich composite structures with exceptional mechanical characteristics for a broad variety of industrial and structural applications.

#### 6.2 Recommendation for Future Works

Increasingly, aeroplanes, ships, and other specialized vehicles are considering sandwich composites for use as structural components, as well. Static and dynamic loads are often applied to sandwich composite structures. In addition, the production of the specimens, particularly the printing of the core, has a substantial effect on the maximum load that may be applied. To reduce this inaccuracy, the production process,

particularly the printing of the core, must be investigated further. More materials, geometric and topological architectures of the core should be studied in the future to combine the deformation of continuous phases to attain greater bending performance. Furthermore, the printed orientation should be studied in the future for more understanding of the effect of printing orientation to the bending behaviour.

In addition, the correctness of the findings from the finite element analysis should be evaluated further. This feature validates the tensile characteristics of materials. Instead of linear structural analysis, the bending behaviour of sandwich composite beams may be analysed utilising nonlinear structural analysis and massive deformation. Increasing the division of cell wall thickness by at least five divisions might result in more precise findings. In further, the model that was utilised in the experiment may have been different from the model that was used in the finite element analysis, which may have had an influence on how accurate the results were. The model may be scanned using a CT scan, and the 3D model can then be imported into a finite element analysis. With the use of this approach, we can certify that the model between the experiment and the finite element will match. In fact, if more accurate findings are desired, more research on the meshing type should be conducted. It is also possible to employ the hexahedral meshing instead of the tetrahedral meshing. Also, the sensitivity of the mesh would impact the accuracy of the results. This may be studied further by executing the convergence test to enhance the mesh's precision and comparing the results to experimental data.

## REFERENCES

- [1] H. Yazdani Sarvestani, A. H. Akbarzadeh, A. Mirbolghasemi, and K. Hermenean, "3D printed meta-sandwich structures: Failure mechanism, energy absorption and multi-hit capability," *Mater Des*, vol. 160, pp. 179-193, Dec, 2018.
- [2] W. Hao, J. Xie, and F. Wang, "Theoretical prediction for large deflection with local indentation of sandwich beam under quasi-static lateral loading," *Compos Struct*, vol. 192, pp. 206-216, May, 2018.
- [3] M. Sun, D. Wowk, C. Mechefske, and I. Y. Kim, "An analytical study of the plasticity of sandwich honeycomb panels subjected to low-velocity impact," *Compos B Eng*, vol. 168, pp. 121-128, Jul, 2019.
- [4] S. V. Iyer, R. Chatterjee, M. Ramya, E. Suresh, and K. Padmanabhan, "A Comparative Study Of The Three Point And Four Point Bending Behaviour Of Rigid Foam Core Glass/Epoxy Face Sheet Sandwich Composites," *Mater Today: Proc*, vol. 5, no. 5, Part 2, pp. 12083-12090, Jan, 2018.
- [5] Z. Li and J. Ma, "Experimental Study on Mechanical Properties of the Sandwich Composite Structure Reinforced by Basalt Fiber and Nomex Honeycomb," *Mater*, vol. 13, p. 1870, Apr, 2020.
- [6] A. Bandyopadhyay, S. Vahabzadeh, A. Shivaram, and S. Bose, "Three-dimensional printing of biomaterials and soft materials," *MRS Bull*, vol. 40, no. 12, pp. 1162-1169, Nov, 2015.
- [7] N. Saad and A. Sabah, *An Investigation of New Design of Light Weight Structure of (ABS/PLA) by Using of Three Dimensions Printing*. 2016.
- [8] L. G. Blok, M. L. Longana, H. Yu, and B. K. S. Woods, "An investigation into 3D printing of fibre reinforced thermoplastic composites," *Addit Manuf*, vol. 22, pp. 176-186, Aug, 2018.
- [9] S. K. Dhinesh, P. S. Arun, K. K. L. Senthil, and A. Megalingam, "Study on flexural and tensile behavior of PLA, ABS and PLA-ABS materials," *Mater Today: Proc*, vol. 45, pp. 1175-1180, Jan, 2021.



- [10] C.-C. Wang, T.-W. Lin, and S.-S. Hu, "Optimizing the rapid prototyping process by integrating the Taguchi method with the Gray relational analysis," *Rapid Prototyp J*, vol. 13, pp. 304-315, Oct, 2007.
- [11] B. M. Tymrak, M. Kreiger, and J. M. Pearce, "Mechanical properties of components fabricated with open-source 3-D printers under realistic environmental conditions," *Mater Des*, vol. 58, pp. 242-246, Jun, 2014.
- [12] K. Morioka and Y. Tomita, "Effect of lay-up sequences on mechanical properties and fracture behavior of CFRP laminate composites," *Mater Charact*, vol. 45, no. 2, pp. 125-136, Aug, 2000.
- [13] J. M. J. F. van Campen, C. Kassapoglou, and Z. Gürdal, "Generating realistic laminate fiber angle distributions for optimal variable stiffness laminates," *Compos B Eng*, vol. 43, no. 2, pp. 354-360, Mar, 2012.
- [14] M. B. Whiteside, S. Pinho, and P. Robinson, "Stochastic failure modelling of unidirectional composite ply failure," *Reliab Eng Syst Saf*, vol. 108, pp. 1–9, Dec, 2012.
- [15] R. Lakes and K. J. Elms, "Indentability of Conventional and Negative Poisson's Ratio Foams," *J Compos Mater*, vol. 27, Jul, 1992.
- [16] L. J. Gibson and M. F. Ashby, *Cellular Solids: Structure and Properties*, 2 ed. (Cambridge Solid State Science Series). Cambridge: Cambridge University Press, 1997.
- [17] T. Li, Y. Chen, X. Hu, Y. Li, and L. Wang, "Exploiting negative Poisson's ratio to design 3D-printed composites with enhanced mechanical properties," *Mater Des*, vol. 142, pp. 247-258, Mar, 2018.
- [18] W. Miller, C. Smith, F. Scarpa, H. Abramovich, and K. Evans, "Multifunctional chiral negative poisson's ratio (auxetic) honeycomb cores with embedded piezo-ceramic patches," Jan, 2009.
- [19] X. Gao, M. Zhang, Y. Huang, L. Sang, and W. Hou, "Experimental and numerical investigation of thermoplastic honeycomb sandwich structures under bending loading," *Thin-Walled Struct*, vol. 155, p. 106961, Oct, 2020.

- [20] K. S. Ashraff Ali, S. Suresh Kumar, J. Allen Jeffrey, M. M. Ravikumar, and S. Rajkumar, "An insight into stress and strain analysis over on hexagonal aluminium sandwich honeycomb with various thickness glass fiber face sheets," *Mater Today: Proc*, vol. 47, pp. 493-499, Jan, 2021.
- [21] S. Upreti, V. K. Singh, S. K. Kamal, A. Jain, and A. Dixit, "Modelling and analysis of honeycomb sandwich structure using finite element method," *Mater Today: Proc*, vol. 25, pp. 620-625, Jan, 2020.
- [22] Z. Li, Z. Wang, X. Wang, and W. Zhou, "Bending behavior of sandwich beam with tailored hierarchical honeycomb cores," *Thin-Walled Struct*, vol. 157, p. 107001, Dec, 2020.
- [23] C. Steeves, "Optimising Sandwich Beams for Strength and Stiffness," *Journal of Sandwich Structures and Materials*, vol. 14, pp. 573-595, 09/01, 2012.
- [24] H. Fukuda, G. Itohiya, A. Kataoka, and S. Tashiro, "Evaluation of Bending Rigidity of CFRP Skin-Foamed Core Sandwich Beams," *Journal of Sandwich Structures and Materials*, vol. 6, pp. 75-92, 01/01, 2004.
- [25] A. Khurram, M. Raza, P. Zhou, and T. Subhani, "A study of the nanocomposite sandwich structures for broadband microwave absorption and flexural strength," *Journal of Sandwich Structures and Materials*, vol. 18, 05/26, 2016.
- [26] A. D. D3039M-17, *Standard Test Method for Tensile Properties of Polymer Matrix Composite Materials*. West Conshohocken, PA, 2017.
- [27] A. D638-14, *Standard Test Method for Tensile Properties of Plastics*. West Conshohocken, PA, 2014.
- [28] A. C. C393M-20, *Standard Test Method for Core Shear Properties of Sandwich Constructions by Beam Flexure*. West Conshohocken, PA, 2020.
- [29] T. S. Lim, C. S. Lee, and D. G. Lee, "Failure Modes of Foam Core Sandwich Beams under Static and Impact Loads," *Journal of Composite Materials*, vol. 38, no. 18, pp. 1639-1662, 2004.
- [30] L. Wahl, A. Zürbes, S. Maas, D. Waldmann, P. Frères, and W. Wintgens, "Fatigue in Aluminium Honeycomb-core Plates," *National Agency for Finite Element Methods*

*and Standards*, pp. 26-32, 01/01, 2011.

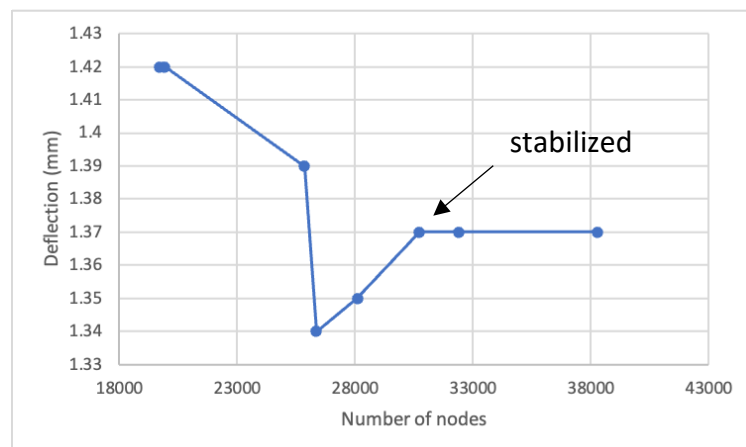


## APPENDIX A

Varying mesh size for body sizing and edge sizing.

Body Sizing			Edge Sizing (Divisions)		Number of Nodes	Number of Elements	Deflection
Face Sheet	Core	Roller	Face Sheet	Core			
8	4	5	2	2	19710	36808	1.4134
8	4	5	3	3	25844	51377	1.3875
8	4	5	4	4	27459	49848	1.3513
8	4	5	5	5	31649	61321	1.3665
7	4	5	2	2	19920	36719	1.4202
7	4	5	3	3	26348	51737	1.3374
7	4	5	4	4	28089	50328	1.3542
7	4	5	4	5	30725	60361	1.3694
7	4	5	5	5	32405	61921	1.3694
6	3	5	5	5	38263	76231	1.3692

A denser element distribution is used to reconstruct the mesh, re-analyse it, and then compare the findings. The final mesh size was chosen when the findings of the deflection has stabilized.

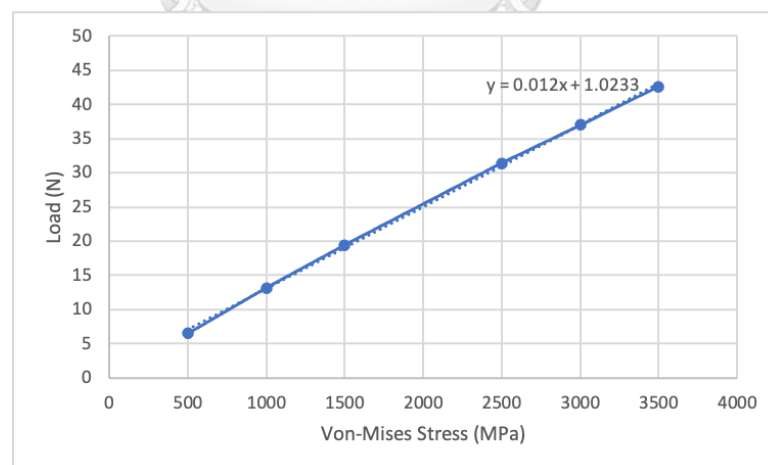


## APPENDIX B

The example of Von-Mises stress of the hexagonal honeycomb core at relative density of 0.3 from finite element analysis.

Load (N)	Von-Mises (MPa)
500	6.51
1000	13.14
1500	19.45
2500	31.37
3000	37.01
3500	42.6

As the yield strength of acrylonitrile butadiene styrene was 44.1 MPa, the maximum load can be determined from the intersection of the linear graph as shown below. Therefore, the maximum load of the hexagonal honeycomb core at relative density of 0.3 was 3589 N.



## VITA

NAME	Dechawat Wannarong
DATE OF BIRTH	17 March 1998
PLACE OF BIRTH	Chonburi, Thailand
INSTITUTIONS ATTENDED	B.Eng. The University of Nottingham, United Kingdom B.Eng. Thammasat University, Thailand
HOME ADDRESS	Bangkok, Thailand

